Excellence in X-ray Detection

Advanced X-ray Cameras for Scientific and Industrial Applications

TELEDYNE
PRINCETON INSTRUMENTS
Everywhereyoulook™

Part of the Teledyne Imaging Group

Table of Contents

Princeton Instruments' 50 Years of Innovation

1961
Introduced VUV coatings and optical filters for aerospace

1979
Introduced research-grade vacuum monochromators

1983
Introduced grazing-incidence spectrometers for soft x-ray / EUV applications

2010
Introduced series of CCD cameras with beryllium window for background reduction, software-selectable readout speeds and gains, thermoelectric cooling, and USB 2.0 (designed for direct detection of x-rays)

2009
Introduced series of fiberoptic-coupled CCD cameras with up to 4k x 4k detection array, thermoelectric cooling, and FireWire® (designed for indirect detection of x-rays)

www.princetoninstruments.com

Engineered for Excellence

For decades, Princeton Instruments has led the way in the development and optimization of innovative camera systems designed to facilitate the most advanced x-ray imaging and x-ray spectroscopy applications. Thousands of these reliable systems continue to prove their outstanding utility and value on a daily basis in a diverse range of scientific and industrial settings worldwide.

Princeton Instruments x-ray camera systems use scientific-grade, two-dimensional CCD detection arrays. Each state-of-the-art solution is engineered with our world-renowned, low-noise analog electronics to support multiple readout speeds and gain architectures.

The faster speeds are useful for alignment, focusing, and rapid data acquisition; the slower speeds are perfect for more precise data collection. The multiple gains, meanwhile, deliver extremely low noise performance or high signal-to-noise ratios.

1992
Introduced soft x-ray CCD cameras

1993
Received patent for special fiberoptic-to-CCD coupling method

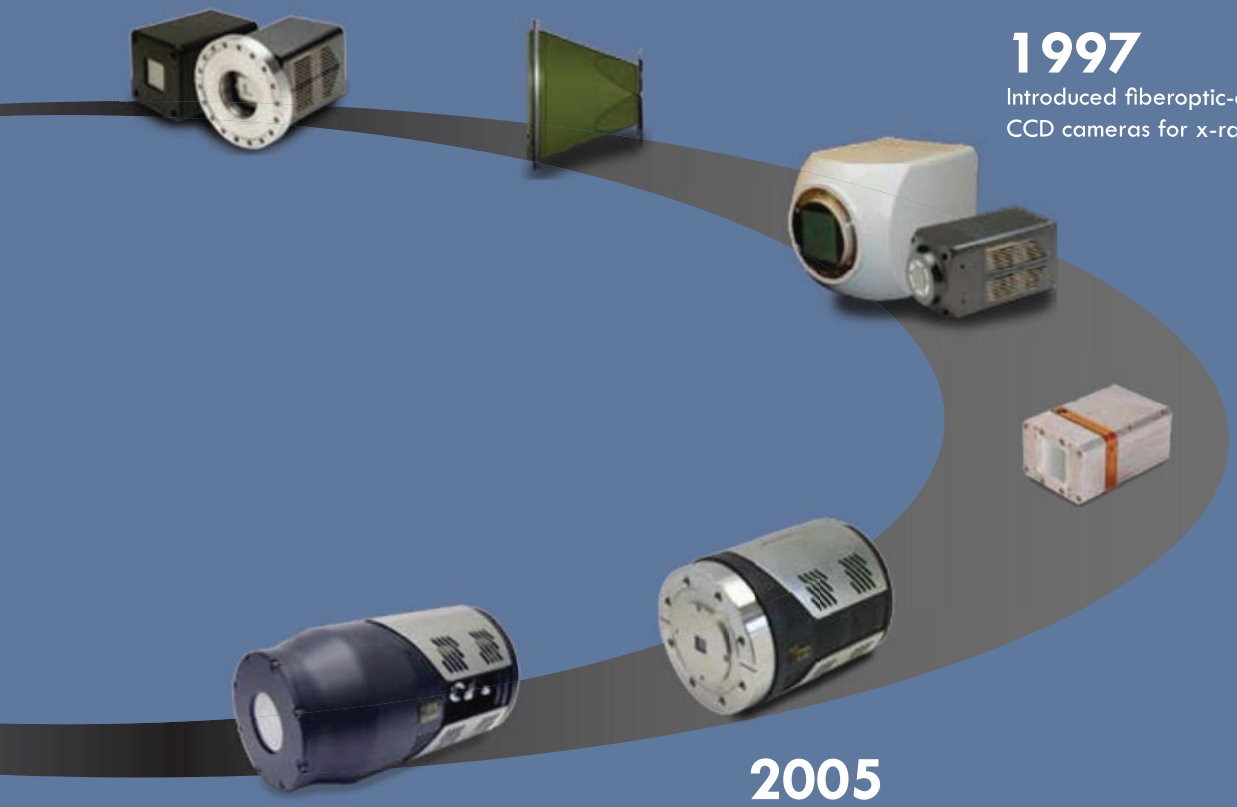

1997
Introduced fiberoptic-coupled CCD cameras for x-ray applications

2000
Introduced world's smallest in-vacuum CCD cameras for direct detection of soft x-rays

2005
Introduced PIXIS® series of CCD cameras with ultradeep cooling, UHV-compatible interface, and USB 2.0 (designed for direct detection of soft x-rays)

2008
Introduced series of fiberoptic-coupled CCD cameras with software-selectable readout speeds and gains, thermoelectric cooling, and USB 2.0 (designed for indirect detection of x-rays)

www.princetoninstruments.com

Our x-ray camera systems feature 16-bit digitization circuits and industry-standard computer interfaces to permit easy integration within experiment setups as well as within larger OEM systems.

Images are transferred from the camera directly to the host computer's memory. In most cases, neither a framegrabber nor any other external digitization hardware is required. Every Princeton Instruments camera system is supplied with all of the hardware and software needed to begin experiments right away!

Princeton Instruments Camera Systems at Synchrotrons Around the World

X-ray cameras from Princeton Instruments are used routinely by researchers at synchrotron radiation facilities around the world. Scientists working in many different disciplines benefit from both the exceptional direct and indirect x-ray detection capabilities offered by our highly versatile, quantitative CCD cameras.

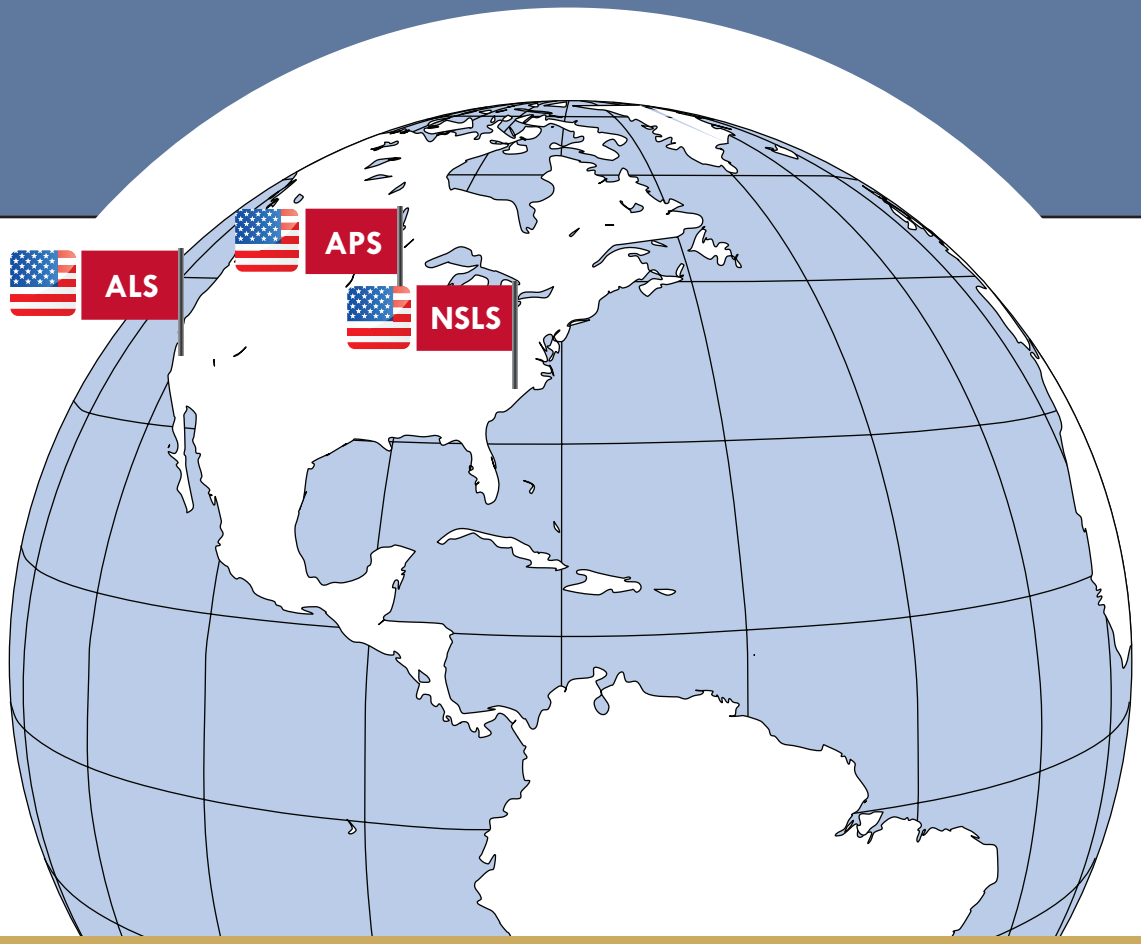

www.princetoninstruments.com

AMERICAS

APS
Argonne, Illinois

NSLS
Upton, New York

ALS
Berkeley, California

ASIA

SSRF
Shanghai, P. R. China

SPring-8 (JASRI)
Harima Science Park City,
Hyogo Prefecture, Japan

Indus-1
Indore, India

The following list is a representative sample of synchrotrons at which Princeton Instruments x-ray cameras provide researchers superior precision, reliability, and performance.

www.princetoninstruments.com

EUROPE

ESRF
Grenoble,
France

Diamond
South Oxfordshire,
England

ELETTRA
Basovizza, Trieste,
Italy

BESSY I / BESSY II
Germany

OCEANIA

Australian Synchrotron
Clayton, Australia

Photos courtesy of respective facilities and agencies.

Selecting the Right Camera

Princeton Instruments realizes that choosing the right x-ray camera system can be a daunting task. The following considerations are integral to an informed selection process:

- Application
- X-ray energy range of interest
- Flux (intensity) of the x-rays reaching the detector
- Required imaging area
- Expected exposure time

With these considerations in mind, begin the search for the right x-ray camera by referring to the charts presented here.

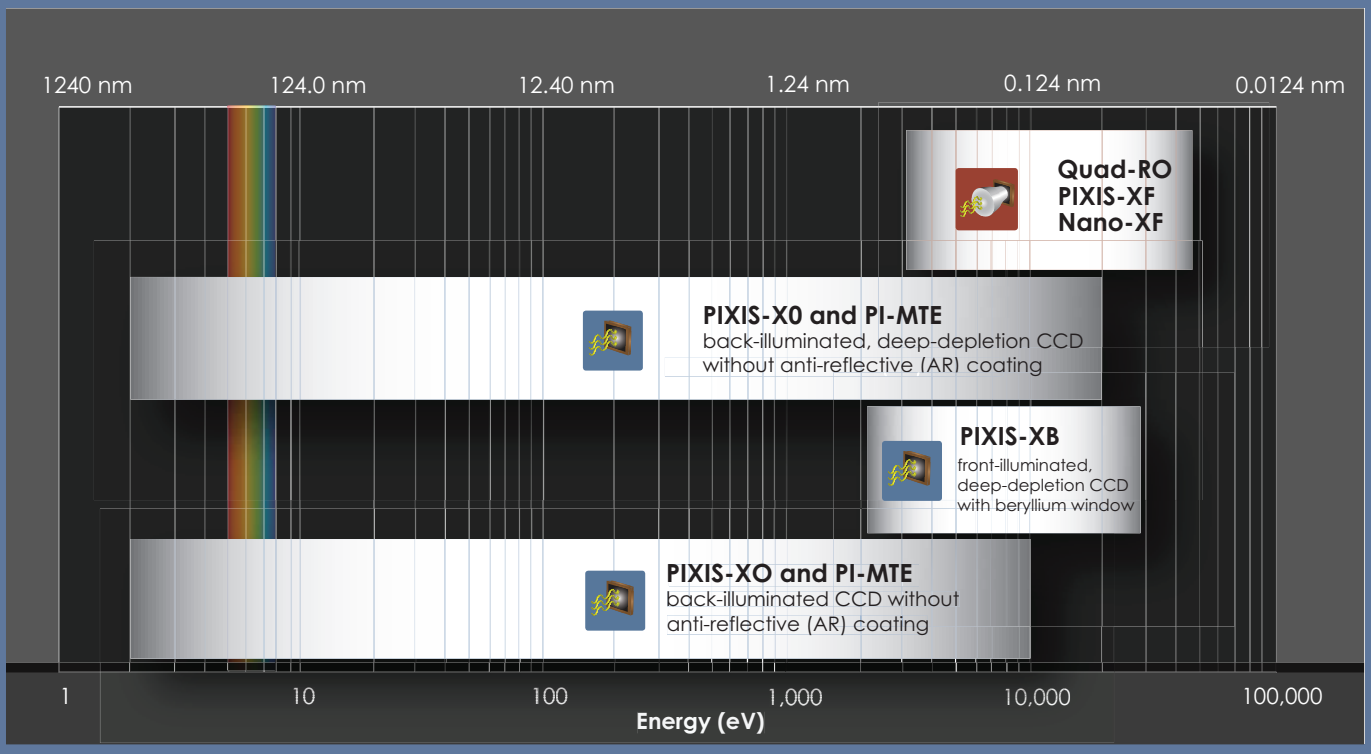

www.princetoninstruments.com

Direct Detection

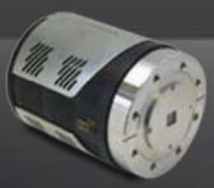

PIXIS-X0
pages 12 - 13

PIXIS-XB
pages 14 - 15

PI-MTE
pages 16 - 17

Energy-to-Wavelength Conversion Chart

x-ray energy (eV) –> wavelength (Å)

eV = 12,400/Å

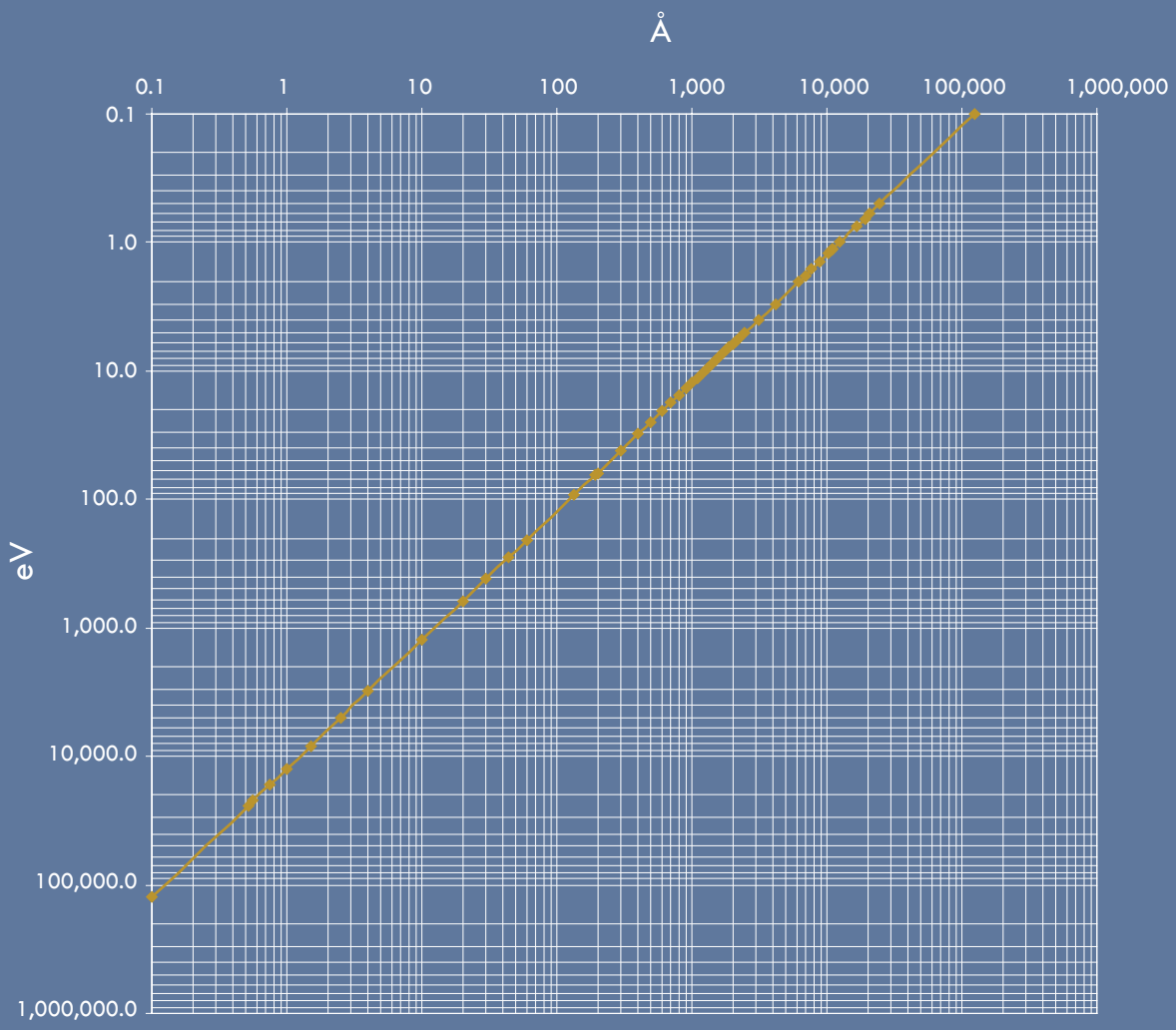

Indirect Detection

Quad-RO
pages 20 - 21

PIXIS-XF
pages 22 - 23

Nano-XF
pages 24 - 25

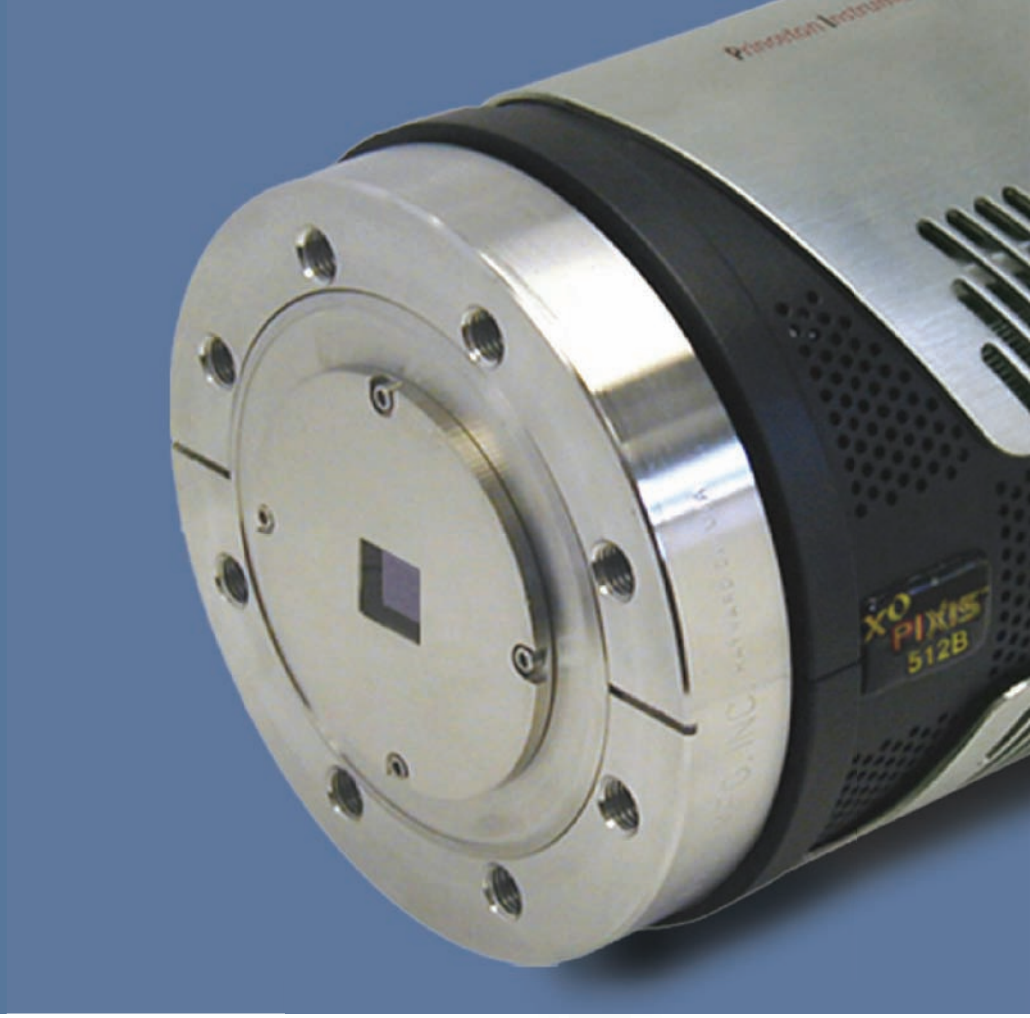

Direct Detection

X-ray Energy	Camera Technologies
< 30 eV to ~ 10 keV	PIXIS-XO with open nose, ConFlat® flange, and back-illuminated NoAR CCDs PI-MTE in-vacuum camera with ST-133 controller and back-illuminated NoAR CCDs
< 30 eV to ~ 20 keV	PIXIS-XO with open nose, ConFlat flange, and back-illuminated deep-depletion CCDs PI-MTE in-vacuum camera with ST-133 controller and back-illuminated deep-depletion CCDs
~ 4 keV to ~ 20 keV	PIXIS-XB with beryllium window PI-MTE in-vacuum camera with ST-133 controller, beryllium window, and deep-depletion CCDs
Phosphor type	*No phosphor required for direct detection*

Direct Detection

In direct-detection cameras, the CCD is directly exposed to incoming x-ray photons, which enables the direct absorption (i.e., detection) of those photons. Depending on the x-ray energy range, these cameras typically utilize either a back-illuminated CCD without anti-reflection coating ("NoAR") or a back- or front-illuminated CCD with deep-depletion technology.

Indirect Detection

X-ray Energy	Camera Technologies
~ 4 keV to ~ 20 keV	PIXIS-XF fiberoptic-coupled camera with back-illuminated or front-illuminated CCDs
~ 4 keV to > 50 keV	Quad-RO fiberoptic-coupled camera with 4-port readout and 2k x 2k or 4k x 4k CCDs
40 kV to 80 kV	Nano-XF fiberoptic-coupled camera with GdOS:Tb phosphor deposited on the fiberoptic
Phosphor type	*GdOS:Tb (contact us for details regarding CsI:Tl)*

Indirect Detection

In indirect-detection cameras, incoming x-rays are absorbed in a polycrystalline or crystalline phosphor. The visible light emitted from this phosphor is channeled through a coherent fiberoptic bundle and subsequently detected by a back-illuminated or front-illuminated CCD. With Princeton Instruments' proprietary bonding process, the fiberoptic is epoxied to the CCD to preserve image quality.

PIXIS-XO

Direct Detection

Camera with ConFlat flange interface for detection of soft x-rays in VUV and EUV applications…

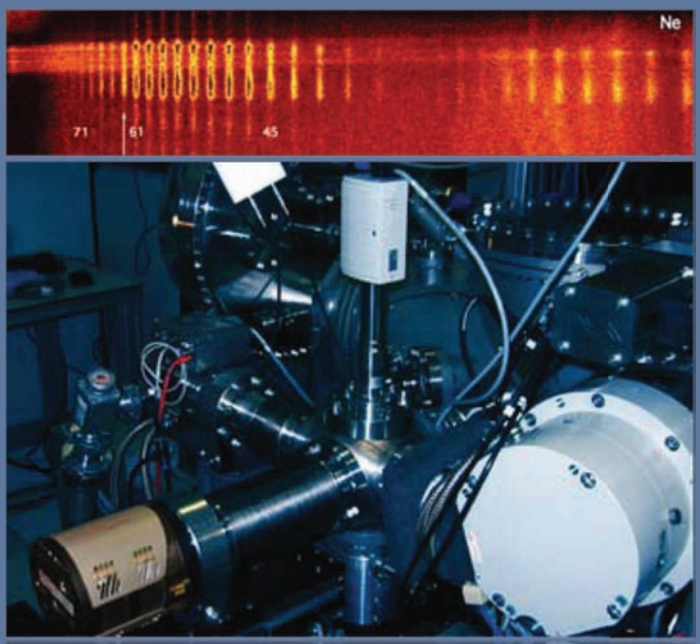

Photo and image courtesy of Prof. Jens Biegert and Stephan Teichmann, The Institute of Photonic Science, Attoscience and Ultrafast Optics, Barcelona, Spain.

< 30 eV to ~ 20 keV

The PIXIS-XO camera utilizes a ConFlat flange to provide a UHV-compatible interface that can achieve vacuum levels below 10^{-6} Torr. Ultradeep thermoelectric cooling and USB 2.0 computer connectivity are incorporated for worry-free operation.

Applications:

EUV lithography

X-ray microscopy

X-ray spectroscopy

X-ray plasma diagnostics

www.princetoninstruments.com

CCD TYPES

actual size

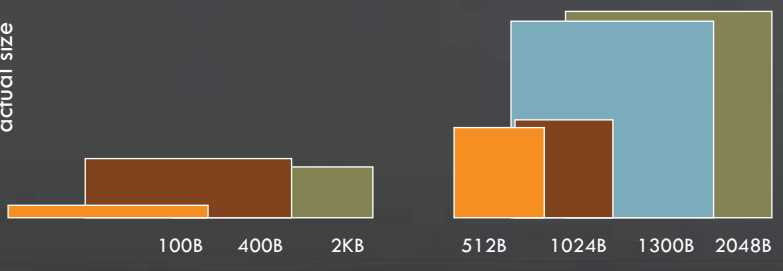

100B	1340 x 100	26.8 mm x 2.0 mm (20 µm pixels)
400B	1340 x 400	26.8 mm x 8.0 mm (20 µm pixels)
2KB	2048 x 512	27.65 mm x 6.9 mm (13.5 µm pixels)
512B	512 x 512	12.28 mm x 12.28 mm (24 µm pixels)
1024B	1024 x 1024	13.31 mm x 13.31 mm (13 µm pixels)
1300B	1340 x 1300	26.8 mm x 26.0 mm (20 µm pixels)
2048B	2048 x 2048	27.65 mm x 27.65 mm (13.5 µm pixels)

FLANGE OPTIONS

6” (ISO 150, DN 100)

4.5” (ISO 100, DN 63)

4.5” removable beryllium window (0.010” / 250 µm) option

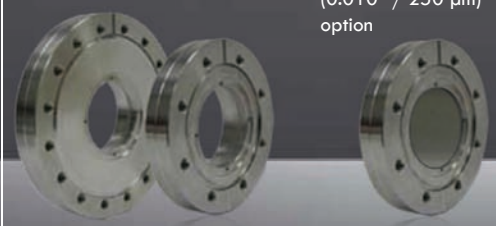

- English thread
- Metric thread
- Through hole option (for 6” flange only)

PIXIS-XO
Direct Detection

- Up to 2048 x 2048 pixels (imaging area: 27.6 x 27.6 mm) available
- Back-illuminated CCDs without anti-reflection coating
- Linux® driver and PICAM/ PVCAM® (64 / 32 bits) DLLs available for custom software development
- Fiberoptic and Ethernet® interfaces available for long-distance camera control
- Available with removable beryllium window flange for worry-free operation in lab
- Easily synchronized with external UniBlitz® puller blade x-ray shutter (up to 30 keV)
- Different sizes and configurations of ConFlat flanges available
- USB 2.0 plug-and-play computer connectivity
- Rotatable ConFlat flange with hard-vacuum seal for 10^{-6} Torr (or better) interface compatibility

www.princetoninstruments.com

OPTIONS & ACCESSORIES

Camera Remote-Operation Kits

USB 2.0 to Fiberoptic

USB 2.0 to Ethernet

Water, air, or LN cooling available

CoolCUBE II

PIXIS-XB

Direct Detection

X-ray camera with beryllium window for low-flux applications…

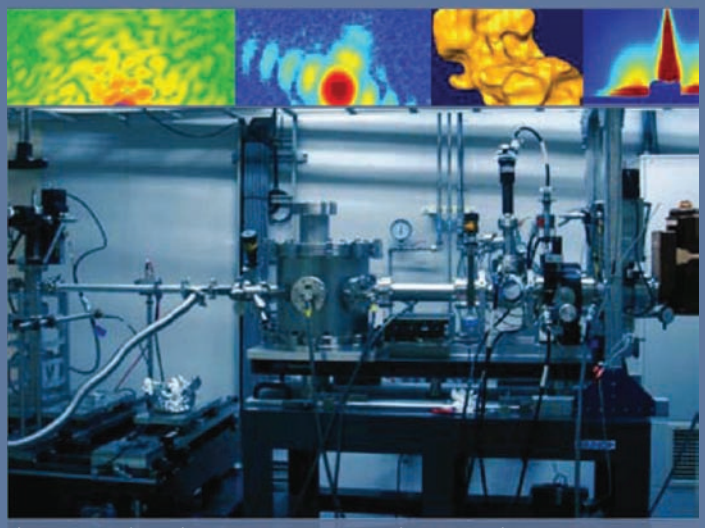

Photo courtesy of Dr. John Miao, UCLA. See page 18 for image credits.

~ 4 keV to ~ 20 keV

The PIXIS-XB camera uses a beryllium window to filter out visible light and low-energy x-rays. This camera does not need to be installed on a vacuum chamber. Deep thermoelectric cooling and USB 2.0 computer connectivity provide worry-free operation.

Applications:

X-ray photon correlation spectroscopy (XPCS)

X-ray intensity fluctuation spectroscopy (XIFS)

X-ray diffraction

X-ray lithography

X-ray spectroscopy

www.princetoninstruments.com

CCD TYPES

actual size

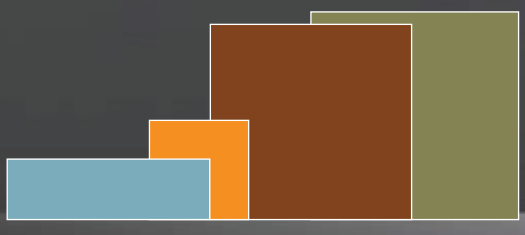

400BR	1340 x 400	26.8 mm x 8.0 mm (20 µm pixels)
1024BR	1024 x 1024	13.31 mm x 13.31 mm (13 µm pixels)
1300R/BR	1340 x 1300	26.8 mm x 26.0 mm (20 µm pixels)
2048BR	2048 x 2048	27.65 mm x 27.65 mm (13.5 µm pixels)

OPTIONS

Beryllium window
size: 0.010" (250 µm)
or 0.020" (500 µm)

Water, air, or LN cooling available

PIXIS-XB
Direct Detection

- Front-illuminated or back-illuminated (without anti-reflection coating) deep-depletion CCDs
- Up to 2048 x 2048 pixels (imaging area: 27.6 x 27.6 mm) available
- Easily synchronized with external UniBlitz puller blade x-ray shutter (up to 30 keV)
- USB 2.0 plug-and-play computer connectivity

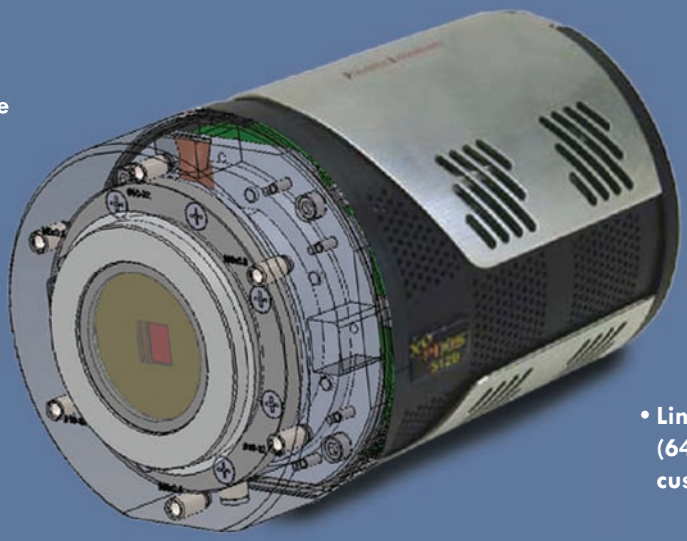

- Mask over CCD protects output amplifier and shift register
- Linux driver and PICAM/ PVCAM (64 / 32 bits) DLLs available for custom software development
- Beryllium window blocks visible light and protects against CCD contamination
- Fiberoptic and Ethernet interfaces available for long-distance camera control

www.princetoninstruments.com

ACCESSORIES

Camera Remote-Operation Kits

USB 2.0 to Fiberoptic

USB 2.0 to Ethernet

CoolCUBE II

PI-MTE

Direct Detection

Small in-vacuum camera for soft x-ray applications…

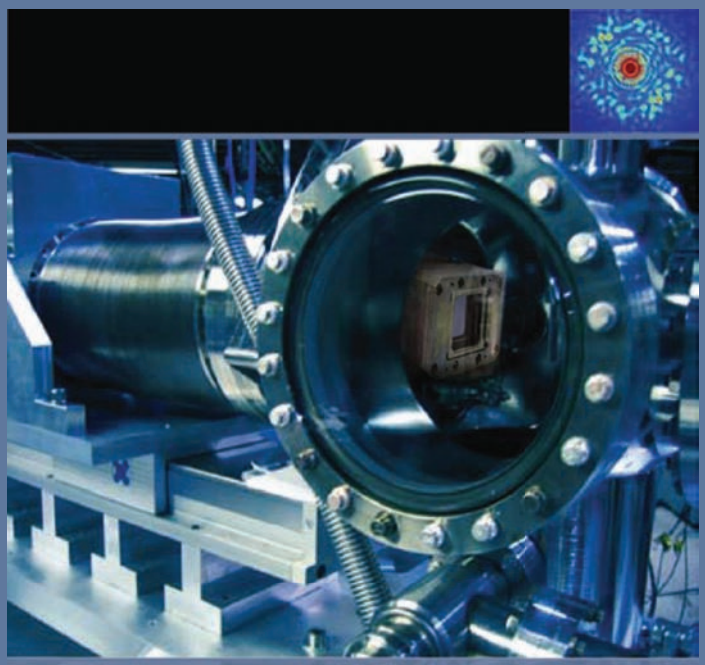

Photo and image courtesy of Jan Luning, SLAC.

< 30 eV to ~ 20 keV

The PI-MTE camera features custom PC boards that are thermally linked to circulating coolant and specially designed for uninterrupted operation inside high-vacuum chambers (~ 10^{-4} Torr) over long periods of time. The camera's lightweight, compact design with flexible liquid and electrical connections facilitates positioning of the detector in limited space or on a movable arm.

Applications:

X-ray microscopy

Soft x-ray imaging

EUV lithography

X-ray plasma imaging

www.princetoninstruments.com

CCD TYPES

actual size

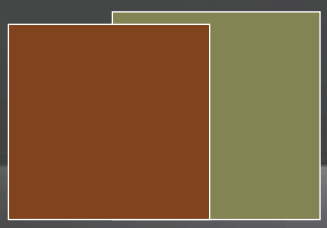

1300B/R/BR 2048B/BR

1300B/R/BR	1340 x 1300	26.8 mm x 26.0 mm (20 µm pixels)
2048B/BR	2048 x 2048	27.65 mm x 27.65 mm (13.5 µm pixels)

OPTIONS

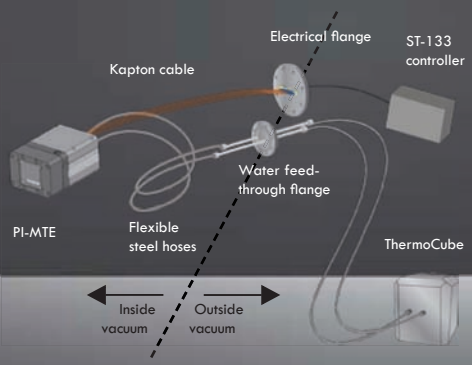

PI-MTE with fiberoptic taper

PI-MTE with deep-depletion CCD

PI-MTE
Direct Detection

- Available with variety of CCD and fiberoptic options
- Up to 2048 x 2048 pixels (imaging area: 27.6 x 27.6 mm) available
- Fiberoptic and Ethernet interfaces available for long-distance camera control
- USB 2.0 plug-and-play computer connectivity
- Easily synchronized with external UniBlitz puller blade x-ray shutter (up to 30 keV) via ST-133 controller

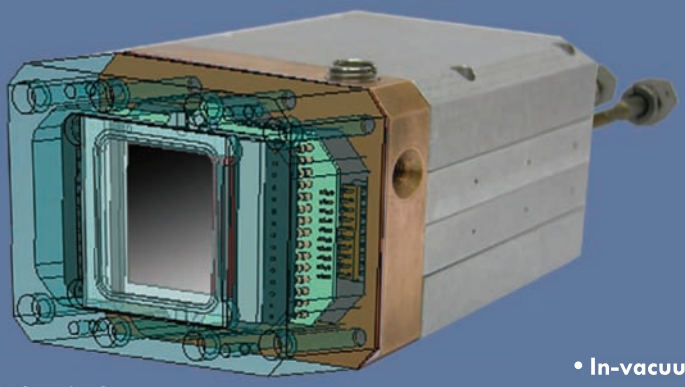

- Linux driver and PICAM/ PVCAM (64 / 32 bits) DLLs available for custom software development
- In-vacuum electrical and liquid connection accessories included
- Available with long external electrical cable – up to 22 feet (6.75 meters)
- Compact design – 3.15" (80 mm) x 2.35" (59.7 mm) x 4.57" (116 mm) and only 2.5 lbs (1.134 kg)
- Specially designed electronics/ PCBs for uninterrupted operation inside vacuum chamber

ACCESSORIES

Electrical feed through ConFlat

Hose feed through ConFlat

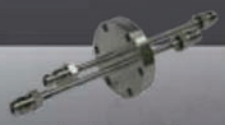

ThermoCUBE

Camera Remote-Operation Kits

USB 2.0 to Ethernet

USB 2.0 to Fiberoptic

Kapton® cable

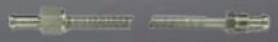

Hose and hose connectors

Direct Detection

CCD Selection Chart

	MODELS	CCD FORMATS (PIXELS)	PIXEL SIZE (µm)	IMAGING AREA (mm x mm)	MAX. COOLING[1]	TYPICAL SYSTEM READ NOISE[2]
PIXIS-XO	100B	1340 x 100	20 x 20	26.8 x 2.0	-80 °C	3.5 e- rms
	400B	1340 x 400	20 x 20	26.8 x 8.0	-75 °C	3.5 e- rms
	2KB	2048 x 512	13.5 x 13.5	27.65 x 6.9	-75 °C	3.5 e- rms
	512B	512 x 512	24 x 24	12.28 x 12.28	-70 °C	5.0 e- rms
	1024B	1024 x 1024	13 x 13	13.31 x 13.31	-70 °C	3.1 e- rms
	1300B	1340 x 1300	20 x 20	26.8 x 26.0	-50 °C	3.5 e- rms
	2048B	2048 x 2048	13.5 x 13.5	27.65 x 27.65	-50 °C	3.5 e- rms
PIXIS-XB	400BR	1340 x 400	20 x 20	26.8 x 8.0	-75 °C	3.5 e- rms
	1300R/BR	1340 x 1300	20 x 20	26.8 x 26.0	-55 °C	3.5 e- rms
	2048BR	2048 x 2048	13.5 x 13.5	27.65 x 27.65	-65 °C	3.5 e- rms
	1024BR	1024 x 1024	13 x 13	13.31 x 13.31	-70 °C	3.1 e- rms
PI-MTE	1300B/R/BR	1340 x 1300	20 x 20	26.8 x 26.0	-50 °C	3.0 e- rms
	2048B/BR	2048 x 2048	13.5 x 13.5	27.65 x 27.65	-50 °C	3.0 e- rms

Specifications subject to change.

1. Max. cooling is specified at an ambient temperature of 20°C.
2. Typical read noise specification is for the entire camera system, not just the CCD. All read noise figures are for 100 kHz readout rate.

B=back illuminated without anti-reflection coating; R=deep depletion; BR=back illuminated, deep depletion

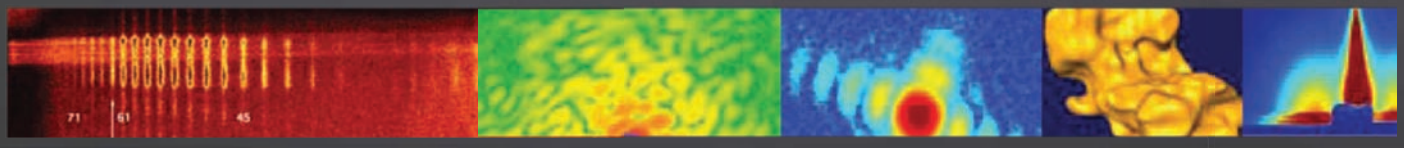

Image courtesy of Prof. Jens Biegert and Stephan Teichmann, The Institute of Photonic Science, Attoscience and Ultrafast Optics, Barcelona, Spain.

Image courtesy of Dr. John Miao, UCLA.

Image courtesy of Dr. I. K. Robinson.

Image courtesy of Dr. John Miao, UCLA.

Image courtesy of Dr. S. Narayanan et al., APS.

TYPICAL BACK-ILLUMINATED (NO-AR COATING) CCD QE CURVE

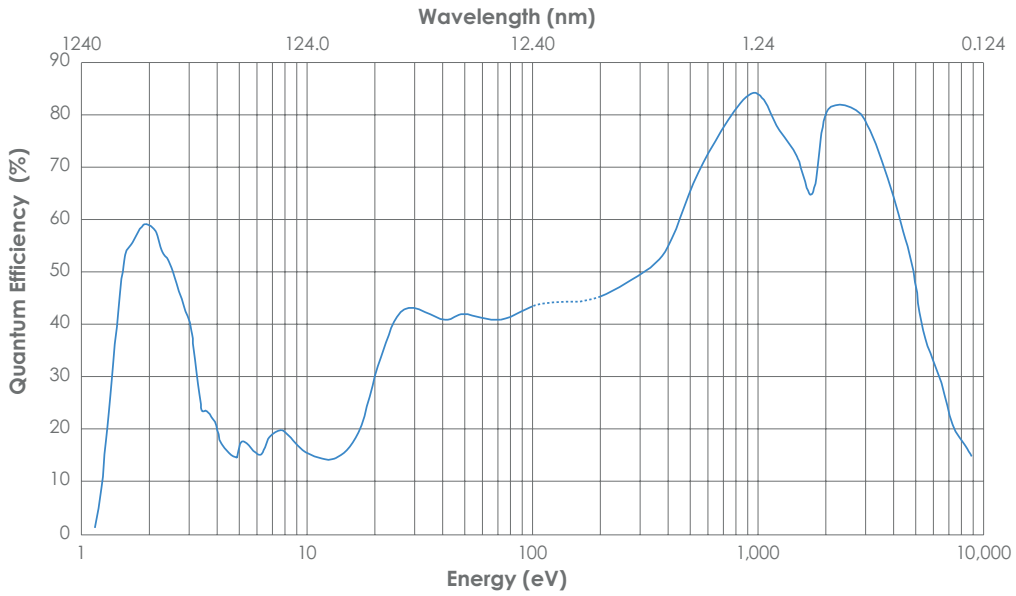

TYPICAL FRONT-ILLUMINATED DEEP-DEPLETION CCD QE CURVE

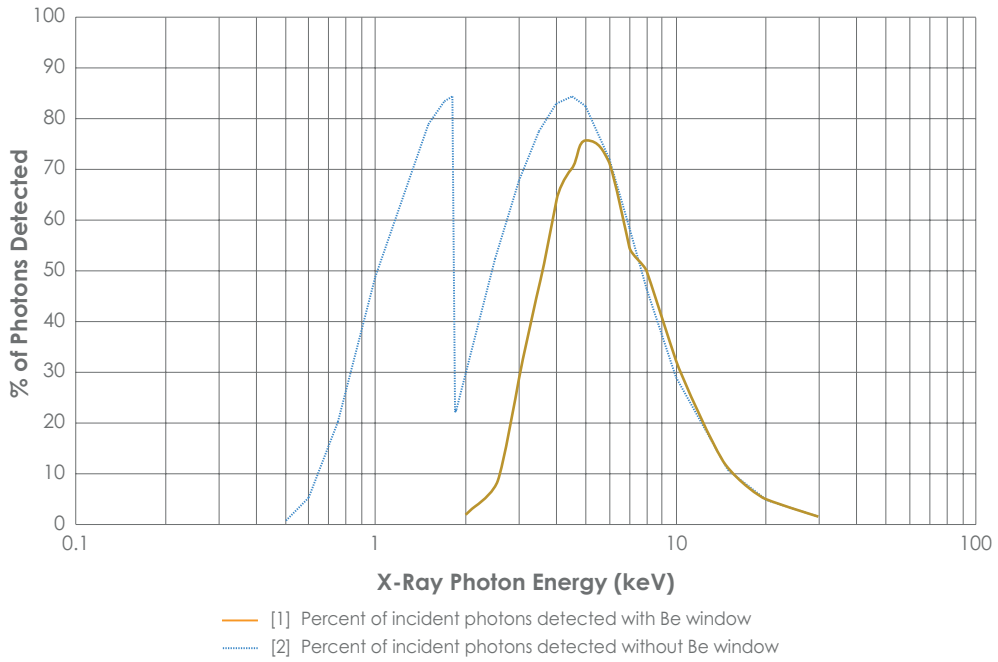

TYPICAL DEEP-DEPLETION, BACK-, FRONT-ILLUMINATED, CCD QE CURVE 250 µM BERYLLIUM WINDOW

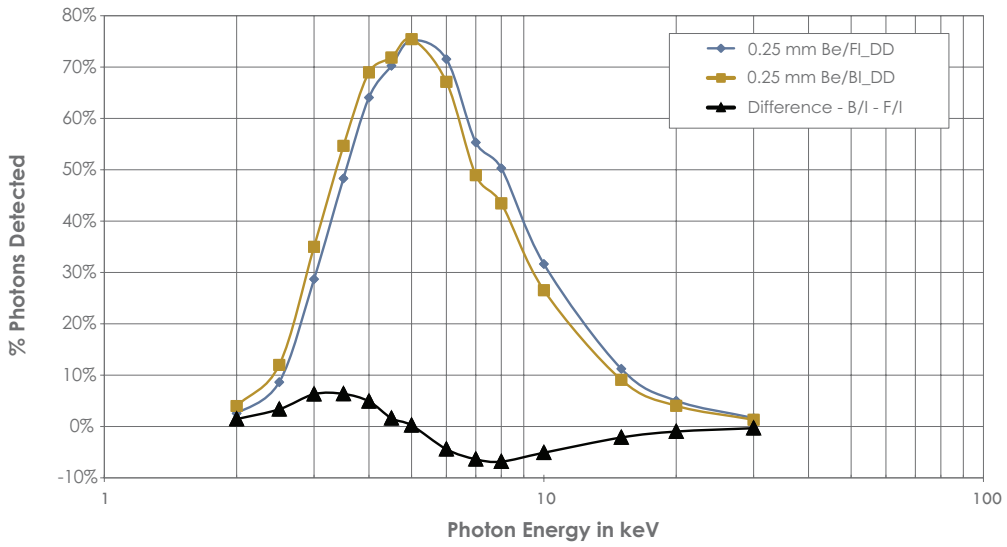

% of incident photons detected with 0.010" (250 µm) thick beryllium window

Quad-RO

Indirect Detection

Large-format camera for x-ray diffraction applications…

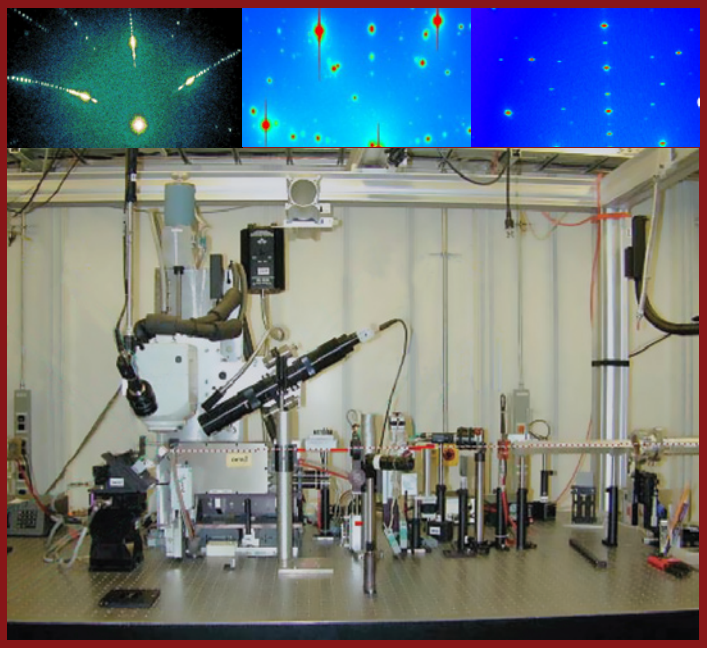

Photo courtesy of Dr. Gene Ice, ORNL. See page 26 for image credits.

~ 4 keV to > 50 keV

The Quad-RO camera features a large-format CCD, either 16 MP or 4 MP (with indium tin oxide technology), as well as multiple-port readout for high-frame-rate imaging. A unique fiberoptic design and several available phosphor options (8 keV, 12 keV, and 17 keV) allow this camera to be easily optimized for specific x-ray energies.

Applications:

X-ray diffraction

X-ray crystallography

X-ray microtomography

X-ray phase contrast imaging

X-ray medical and industrial imaging

CCD TYPES

actual size

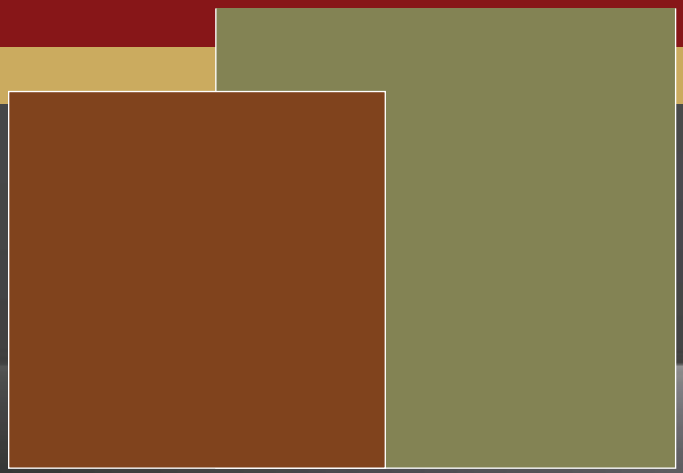

4320	2084 x 2084	50.0 mm x 50.0 mm (24 µm pixels)
4096	4096 x 4096	61.44 mm x 61.44 mm (15 µm pixels)

OPTIONS

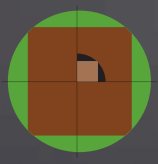

4320 with 165 mm fiberoptic taper provides 120 x 120 mm image area

4096 with 165 mm fiberoptic taper provides 160 mm circular image area

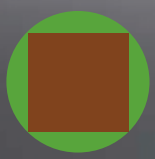

4320 with 1:1 fiberoptic provides 50 x 50 mm image area; 4096 with 1:1 fiberoptic provides 60 x 60 mm imaging area

Quad-RO
Indirect Detection

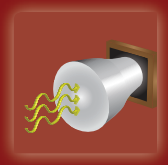

- **Up to 4096 x 4096 pixels (imaging area: 61.44 x 61.44 mm) available**
- **Electronically balanced quadrants deliver an extremely uniform raw image**
- **Front-illuminated CCDs with indium tin oxide (70% QE @ 550 nm to deliver the highest sensitivity)**
- **FireWire (IEEE 1394a) computer connectivity**
- **Distortion correction software available**
- **Low-noise, 4-port readout (single-port readout available)**
- **Available with long signal and power cables (75 feet / 23 meters) to keep heat outside x-ray hutch**
- **Unique mechanical design with fiberoptic extended outside vacuum allows performance optimization with custom phosphor screens**
- **Linux driver and PICAM/ PVCAM (64 / 32 bits) DLLs available for custom software development**

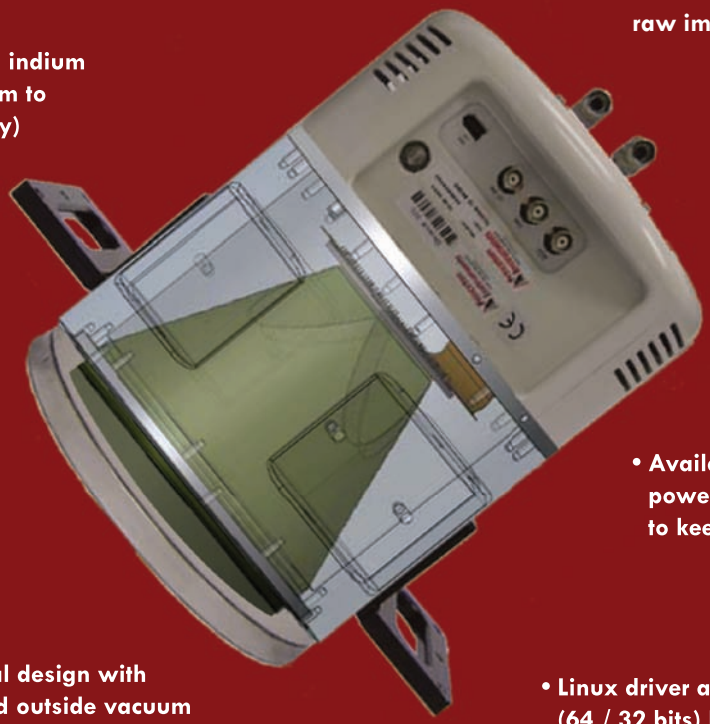

www.princetoninstruments.com

ACCESSORIES

- GdOS:Tb phosphors available for 8, 12, or 17 keV (emission wavelength: 550 nm)

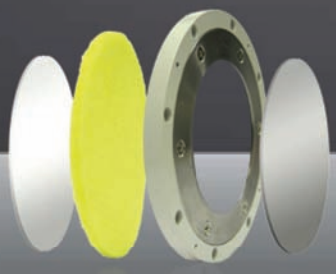

- Contact us for details regarding CsI:Tl phosphor availability

Camera Remote-Operation Kit

ThermoCUBE

FireWire to Fiberoptic

PIXIS-XF

Indirect Detection

X-ray camera for medium-energy applications…

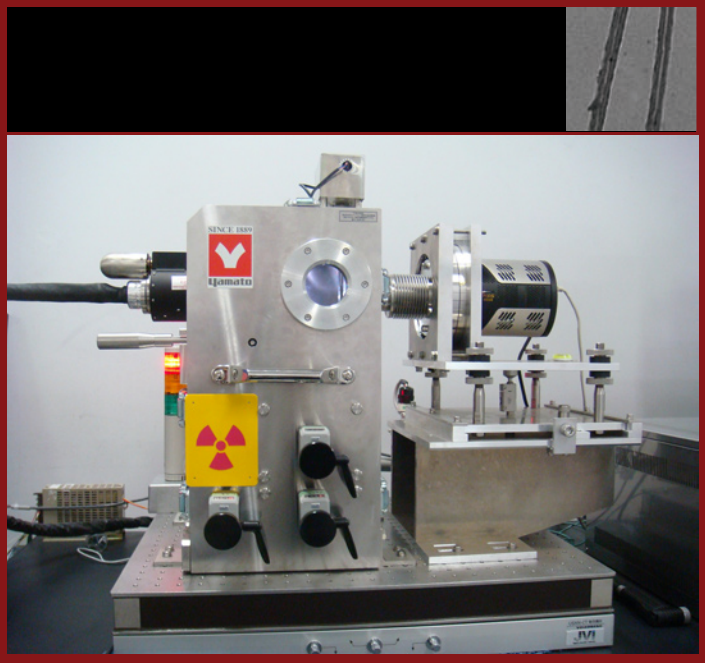

Photo and image courtesy of K. Murata, Yamato Scientific Co., Ltd.

~ 4 keV to ~ 20 keV

The PIXIS-XF camera, which is offered with up to a 4 MP CCD, is designed for medium-energy x-ray applications. A unique fiberoptic design and several available phosphor options allow this camera to be easily optimized for specific x-ray energies. The 1:1 fiberoptic ratio and 13 µm pixel size of the 1 MP CCD camera model offers resolution of ~ 38 lp/mm.

Applications:

X-ray computed microtomography

Streak tube and CRT readout

Industrial and medical imaging

www.princetoninstruments.com

CCD TYPES

actual size

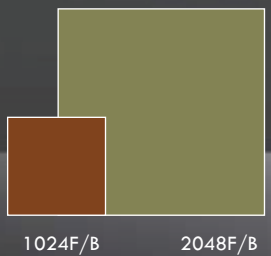

1024 F/B	1024 x 1024	13.31 mm x 13.31 mm (13 µm pixels)
2048 F/B	2048 x 2048	27.65 mm x 27.65 mm (13.5 µm pixels)

OPTIONS

- GdOS:Tb phosphors available for 8 or 17 keV (emission wavelength: 550 nm)
- Contact us for details regarding CsI:Tl phosphor availability

PIXIS-XF

Indirect Detection

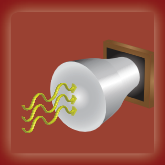

- Up to 2048 x 2048 pixels (imaging area: 27.6 x 27.6 mm) available
- Back- and front-illuminated CCDs
- Custom fiberoptic taper configurations
- Easily synchronized with external UniBlitz puller blade x-ray shutter (up to 30 keV)

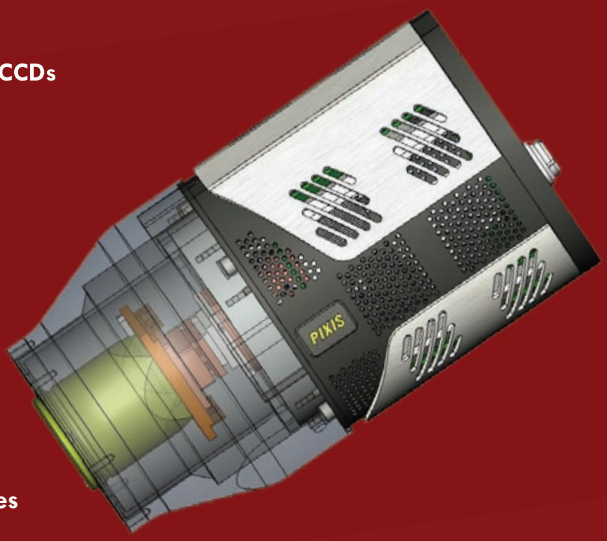

- USB 2.0 plug-and-play computer connectivity
- Fiberoptic and Ethernet interfaces available for long-distance camera control
- Unique mechanical design with fiberoptic extended outside vacuum allows performance optimization with custom phosphor screens
- Linux driver and PICAM/ PVCAM (64 / 32 bits) DLLs available for custom software development

www.princetoninstruments.com

ACCESSORIES

Camera Remote-Operation Kits

USB 2.0 to Fiberoptic

USB 2.0 to Ethernet

CoolCUBE II

Nano-XF

Indirect Detection

High-resolution camera for industrial x-ray applications…

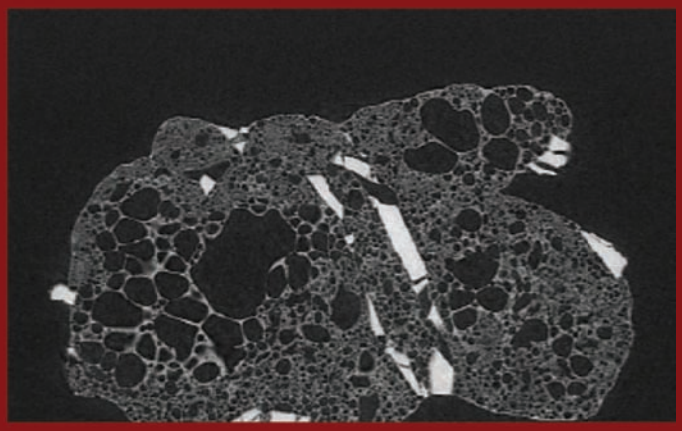

Image courtesy of Liping Bai and Don Baker, Earth and Planetary Sciences, McGill University, Montreal, Canada, and Dr. Mark Rivers, University of Chicago.

40 kV to 80 kV

The Nano-XF camera provides 11 MP resolution and is designed for industrial x-ray applications. Its 1.4:1 fiberoptic taper ratio (with phosphor deposited directly on the taper) enables the camera to provide a 50 mm x 33 mm field of view.

Applications:

X-ray computed microtomography

X-ray medical and industrial imaging

www.princetoninstruments.com

CCD TYPES

actual size

11000

11000 | 4008 x 2672 | 36.0 mm x 24.0 mm (9 µm pixels)

Nano-XF

Indirect Detection

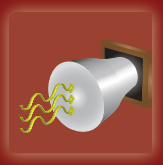

- 4008 x 2672 pixels (imaging area: 36 x 24 mm)
- Front-illuminated, interline-transfer CCD with indium tin oxide
- GdOS:Tb phosphor deposited on the fiberoptic
- Delivers up to 4.63 full frames per second
- 1.4:1 fiberoptic (field of view: 50 x 33.3 mm)
- High sensitivity and wide dynamic range
- Compact design – 3.75" (95 mm) x 3.75" (95 mm) x 6.66" (169 mm) and 4.5 lbs (2.05 kg)

Controller

Indirect Detection

CCD Selection Chart

	MODELS	CCD FORMATS (PIXELS)	PIXEL SIZE (µm)	IMAGING AREA (mm x mm)	MAX. COOLING[1]	TYPICAL SYSTEM READ NOISE[2]
Quad-RO	4096 4320 (ITO)	4096 x 4096 2084 x 2084	15 x 15 24 x 24	61.44 x 61.44 50 x 50	-45 °C -45 °C	9 e- rms @ 500 kHz 8 e- rms @ 500 kHz
PIXIS-XF	1024F/B 2048F/B	1024 x 1024 2048 x 2048	13 x 13 13.5 x 13.5	13.31 x 13.31 27.65 x 27.65	-40 °C -40 °C	3.1 e- rms @ 100 kHz 3.5 e- rms @ 100 kHz
Nano-XF	11000	4008 x 2672	9 x 9	36 x 24	-15 °C	20 e- rms @ 30 MHz

Specifications subject to change.
1. Max. cooling is specified at an ambient temperature of 20°C.
2. Typical read noise specification is for the entire camera system, not just the CCD.
F=front illuminated; B=back illuminated

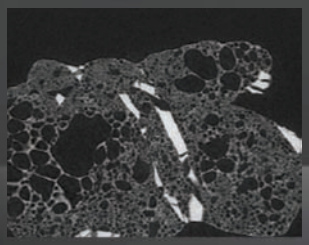

Image courtesy of Liping Bai and Don Baker, Earth and Planetary Sciences, McGill University, Montreal, Canada, and Dr. Mark Rivers, University of Chicago.

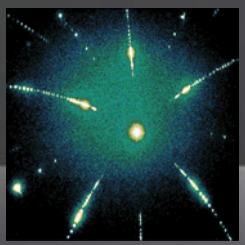

Image courtesy of Dr. Gene Ice, Oak Ridge National Laboratory (ORNL), Oak Ridge, TN, USA.

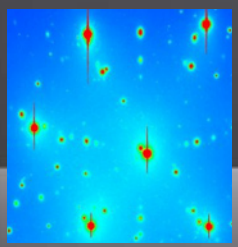

Image courtesy of S.M. Polvino and H. Yan, Department of Applied Physics and Applied Math, Columbia University, New York, NY.

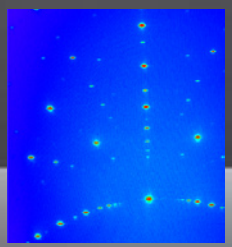

Image courtesy of S.M. Polvino and H. Yan, Department of Applied Physics and Applied Math, Columbia University, New York, NY.

KODAK® ITO CCD QE CURVE

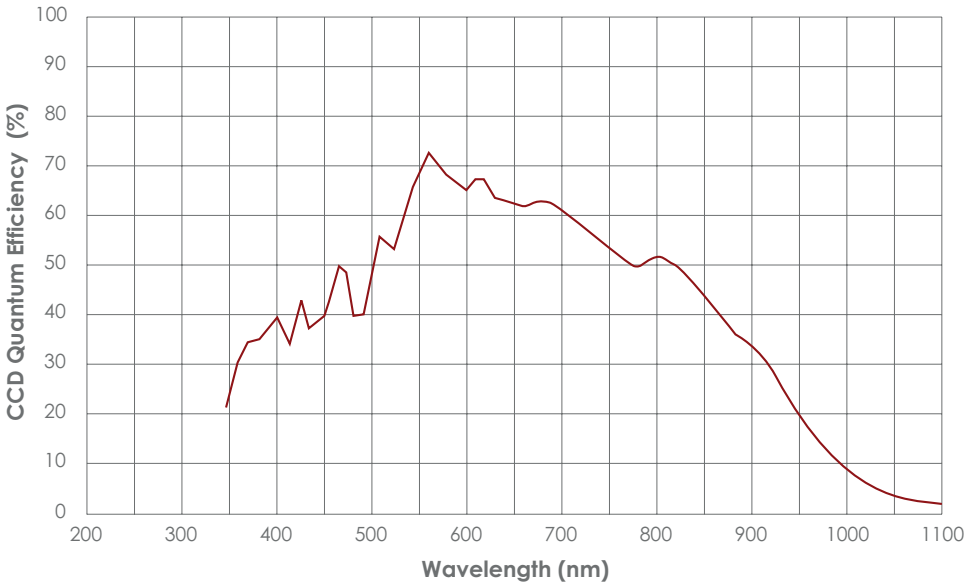

FRONT- AND BACK-ILLUMINATED CCD QE CURVE

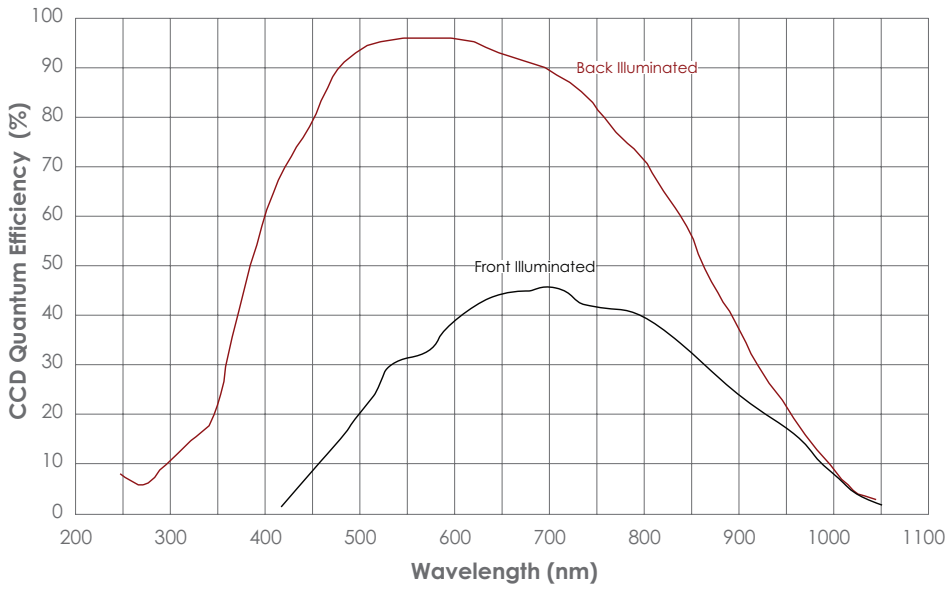

KODAK INTERLINE CCD QE CURVE

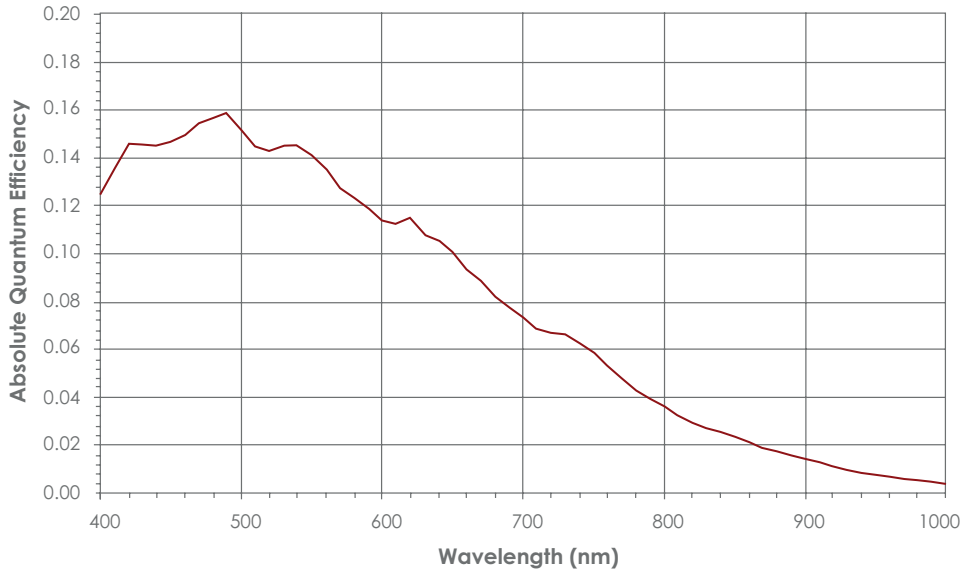

Options and Accessories

COOLING

CoolCUBE II

The CoolCUBE II is a compact liquid circulator designed for use with PIXIS-XO, PIXIS-XB, and PIXIS-XF cameras. This self-contained unit provides liquid circulation for efficient cooling and is ideal for applications that require vibration-free and/or thermally stable environments free of air currents. Setup is easy using the circulator's no-spill, quick-disconnect fittings.

COOLING

ThermoCUBE

The ThermoCUBE is a compact liquid chiller designed for use with Quad-RO and PI-MTE cameras. Its self-contained reservoir provides liquid circulation for deep, efficient cooling performance. The chiller is perfect for applications that demand vibration-free and/or thermally stable environments. Connectivity (via hose barb fitting) is quick and simple.

INDIRECT DETECTION

Phosphor Kits

The performance of Quad-RO and PIXIS-XF indirect-detection cameras can be optimized by selecting the right GdOS:Tb phosphor for the x-ray energy range of interest. In addition, the design of these cameras allows users to switch/replace the phosphor quickly and easily.

Each phosphor kit includes all required mechanical components, including a beryllium window and a GdOS:Tb phosphor. Currently, GdOS:Tb phosphors for 8 keV, 12 keV, and 17 keV are offered. For other energies, please contact a Princeton Instruments sales representative.

CAMERA REMOTE-OPERATION KITS

USB 2.0 to Fiberoptic

This remote-operation (extender) kit allows PIXIS-XO, PIXIS-XB, PIXIS-XF, and PI-MTE cameras to be separated by up to 500 meters from a host computer without any loss of data. The easy-to-install kit consists of two compact, high-speed transceivers (interface modules) for completely transparent operation between computer and camera. It is ideal for use in hazardous or high-EMI environments.

CAMERA REMOTE-OPERATION KITS

USB 2.0 to Ethernet

This remote-operation (extender) kit allows PIXIS-XO, PIXIS-XB, PIXIS-XF, and PI-MTE cameras to be separated by up to 100 meters from a host computer without any loss of data via Ethernet. It is well suited for use in hazardous or high-EMI environments.

CAMERA REMOTE-OPERATION KITS

FireWire to Fiberoptic

This remote-operation (extender) kit allows Quad-RO cameras to be separated by up to 1000 meters from a host computer without any loss of data using a multimode fiberoptic cable. The plug-and-play kit is compact and easy to install. It is ideal for use in hazardous or high-EMI environments.

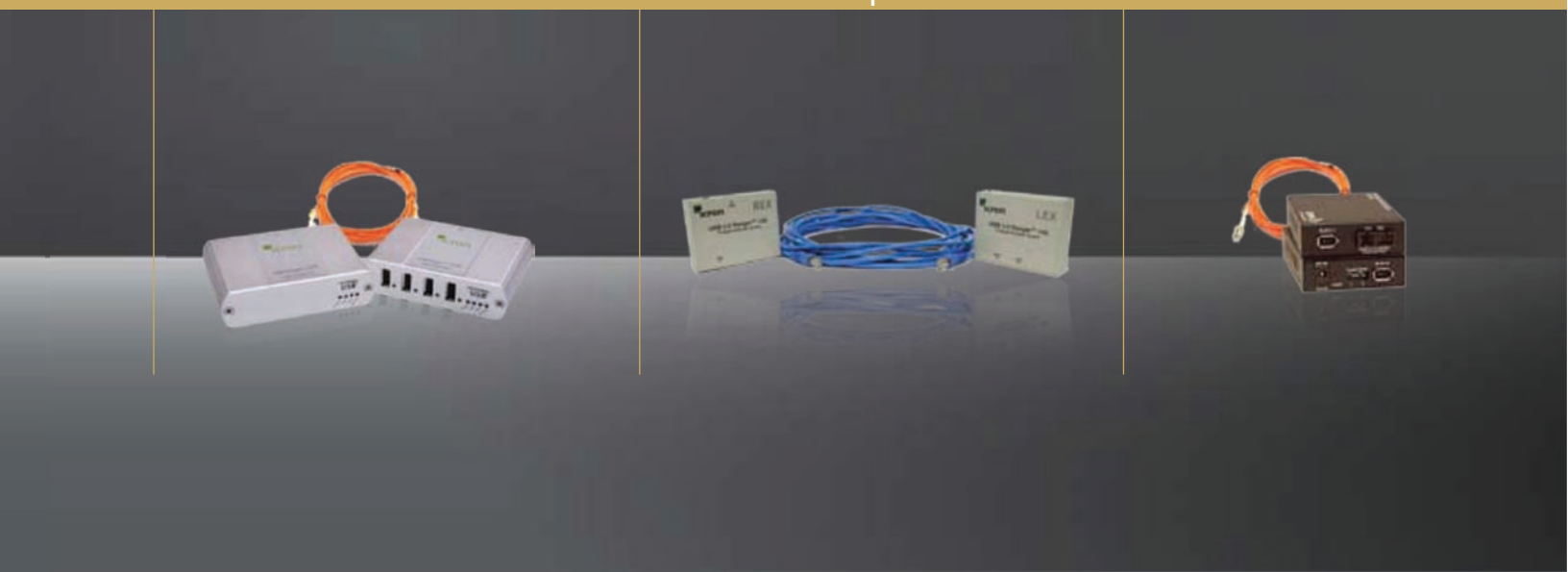

Software | LightField

True 64-bit Data Acquisition Software

Princeton Instruments LightField is a new 64-bit data acquisition software platform that runs under Microsoft® Windows® 7 and has been designed for use in x-ray imaging and x-ray spectroscopy applications. It provides comprehensive control of Princeton Instruments Quad-RO, PIXIS-XO, PIXIS-XB, and PIXIS-XF cameras via easy-to-use tools that help streamline experimental setup, data acquisition, and post processing.

Data integrity is LightField's top priority. The new platform automatically saves data to disc during acquisition, applies a time stamp, and retains both raw and corrected data in the resultant file along with full experimental details.

LightField is an excellent solution for multi-user facilities. The platform remembers each user's hardware and software configurations and tailors its own features accordingly, displaying all relevant tools via an intuitive graphical user interface.

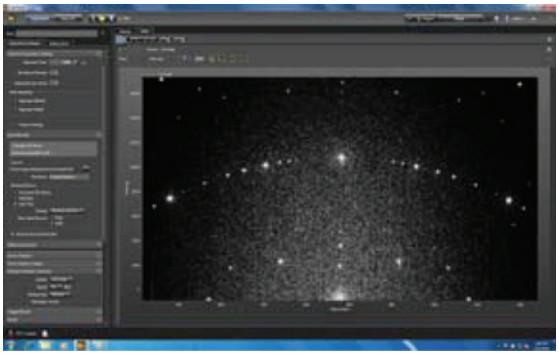

Salient features:

- Cutting-edge user interface
- Built for latest generation of multi-core 64-bit processors
- Progressive disclosure; contextual menus ensure that only relevant options appear
- Stream thousands of images and gigabytes of data to hard drive
- All experimental parameters saved to data file headers; no more searching old notebooks for data acquisition settings
- Automatic light saturation warning with pseudocolor

Software | WinSpec / WinView

32-bit Data Acquisition Software

Princeton Instruments WinSpec and WinView each offer scientists a complete, off-the-shelf package that includes real-time data acquisition, display, post-acquisition processing, data manipulation, and archiving capabilities. Users gain unparalleled benefits from their high-performance Princeton Instruments x-ray cameras and reliable control over experimental parameters.

From the installation process to everyday experimental acquisition, WinSpec and WinView provide an intuitive, easy-to-use interface, helping researchers obtain valuable results in a simple and efficient manner. The unique hardware wizard allows users to set up and test their system instantly. Since all experimental parameters can be easily accessed via a single dialog box, it is possible to have an experiment up and running in minutes.

The sophisticated flexibility of the software package means that customer-written and compiled software modules can be incorporated. These modules are accessed as dynamic link libraries (DLLs) and provide a set of simple commands for programmers to write custom software for controlling Princeton Instruments x-ray camera systems. Built-in functions handle hardware configuration, high-speed data transfer, and large-volume memory management, making it easy to develop custom Windows software.

Salient features:

- Comprehensive support of Princeton Instruments x-ray camera hardware and advanced acquisition capabilities
- 1D, 2D, and 3D image display modes
- File format support for SPE, TIF, ASCII, and FITS
- Full suite of image filters and math functions
- Macro-record feature for easy automation of repetitive tasks
- Visual Basic® interface for easy customization and online data processing

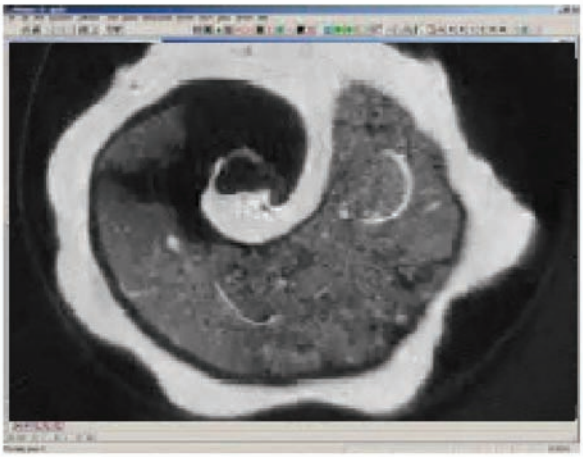

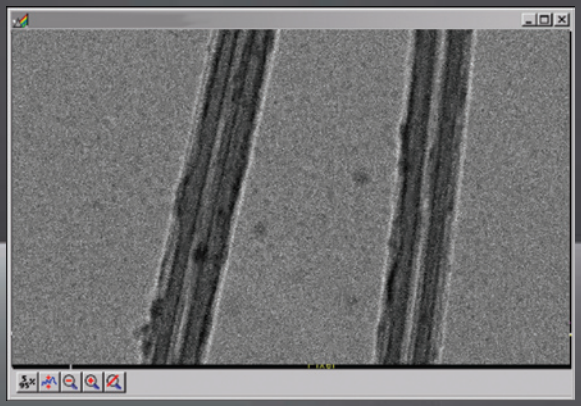

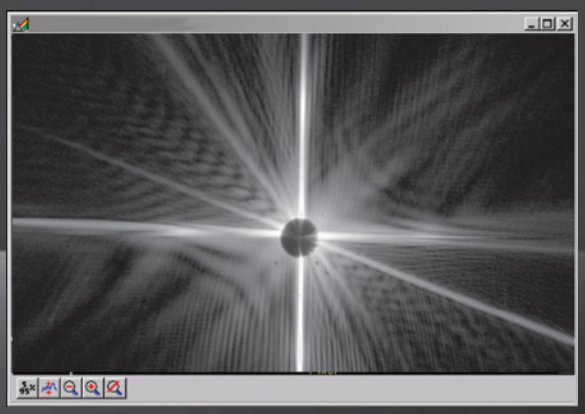

“Distortion Correction” Software

The Problem

When an indirect-detection camera is manufactured with a fiberoptic taper, certain types of distortions (e.g., geometric distortion, shear distortion, and circular distortion) are introduced. Distortions often prove particularly challenging for applications involving x-ray µCT and x-ray diffraction imaging. These distortions deform the original image when digitized, ultimately leading to the presence of artifacts and errors in the final results; geometric distortion is commonly the main culprit. To create the best image, it is very important to remove such artifacts and errors. Princeton Instruments “Distortion Correction” software achieves this via the use of a software “SnapIn”.

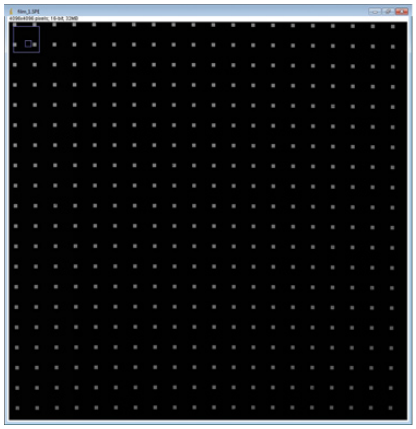

The Solution

First, a special type of “Grid Mask” developed by Princeton Instruments is imaged. Using this Grid Mask image along with a uniform x-ray intensity image, a “Distortion and Flat Field Correction” file (unique to each camera) is created and supplied to the user.

By utilizing the software SnapIn and the unique Distortion Correction file either online or offline (i.e., post processing), distortion and flat field correction can be applied to all images.

Refer to the fiberoptics section found later in this brochure for more information about distortions.

EXAMPLE

The following image pair demonstrates how the Distortion Correction algorithm works.

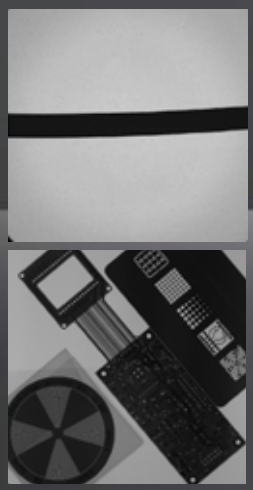

Uncorrected sample

Corrected sample

Software

PICAM/PVCAM

Princeton Instruments PICAM (64 bits) / PVCAM (32 bits) allows users to control the complete range† of Princeton Instruments x-ray cameras. This universal programming interface is a custom, ANSI C library that is used to create the camera control and data acquisition interface. It contains a suite of functions that allow configuration of the data acquisition process in a number of different ways as well as control of standard camera functions such as temperature and shutter operation. PICAM/PVCAM can be used with a wide variety of programming environments, including C, C++, Visual Basic, and LabVIEW.

- Support for Windows* and Linux*
- Universal API calls for hardware virtualization
- Full support of hardware functionality
- Simplified function calls
- Comprehensive suite of programming examples

†*The PI-MTE camera is supported by PVCAM, but not PICAM.*

**Contact Princeton Instruments about the latest supported hardware.*

LabVIEW™ SITK

This scientific imaging tool kit (SITK) provides prewritten virtual instrument (VI) modules to quickly integrate camera functions into a larger experimental setup using National Instruments LabVIEW. Customers do not have to create the VIs from the ground up, saving valuable research time.

- Prewritten VI modules provide full control over Princeton Instruments x-ray camera hardware and advanced acquisition capabilities
- Advanced display control
- Background and flat field corrections
- Support for advanced features such as kinetics, custom chip, and timing

Linux

The Linux driver enables control of all new Princeton Instruments x-ray cameras through the PICAM/PVCAM software development kit.

- Full support of hardware functionality
- Comprehensive suite of programming examples
- Source code available at no charge

All new Princeton Instruments x-ray cameras include the Linux driver and support kernel 2.6.19 or later. Note that Fedora® 12, openSUSE® 11.2, Ubuntu® 8.0 LTS, and Mandriva® distributions have been tested successfully on the Quad-RO camera.

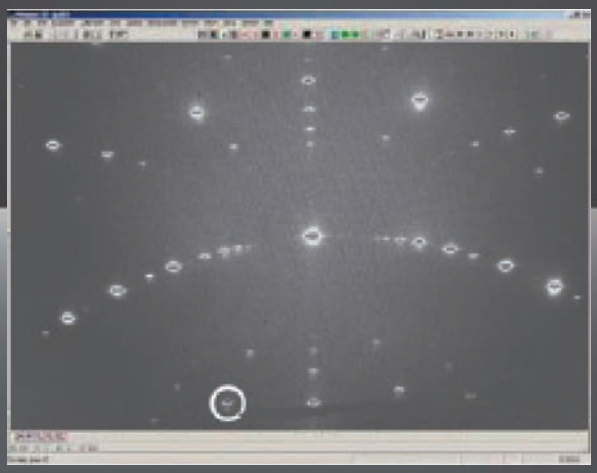

TECHNICAL BRIEFS

Energy Resolution in Direct-Detection Cameras

Many parameters must be considered to ensure that the theoretical energy resolution of a direct-detection CCD camera is realized. A few of the most important factors for achieving the highest energy resolution are the right type of CCD, the best charge transfer efficiency (CTE), the lowest thermal noise, and linear response throughout the entire dynamic range. Princeton Instruments x-ray cameras use scientific-grade CCDs and world-renowned low-noise electronics to optimize these parameters.

Assuming the best performance from the camera, the average energy required to create 1 e-h pair in the CCD is ~ 3.65 eV/e-. Only considering single-pixel events (i.e., ignoring any split-pixel events and electron loss in the field-free substrate), the energy resolution in "eV" can be calculated as:

$$R(E) = 3.65\ (eV/e\text{-}) * 2.355 * \sqrt{[f * N(e\text{-}) + RN\ (e\text{-})^2]}$$

Where:

R(E) = Energy resolution in eV

N(e-) = Number of electrons generated in the CCD for a given x-ray energy

E = E (eV) / 3.65 (eV/e-)

RN(e-) = CCD RMS read noise

f = Fano factor = An empirically derived factor by which the variance of generated e- (by the primary x-ray photon) is reduced from the expected random distribution. The Fano factor is 0.12 in silicon.

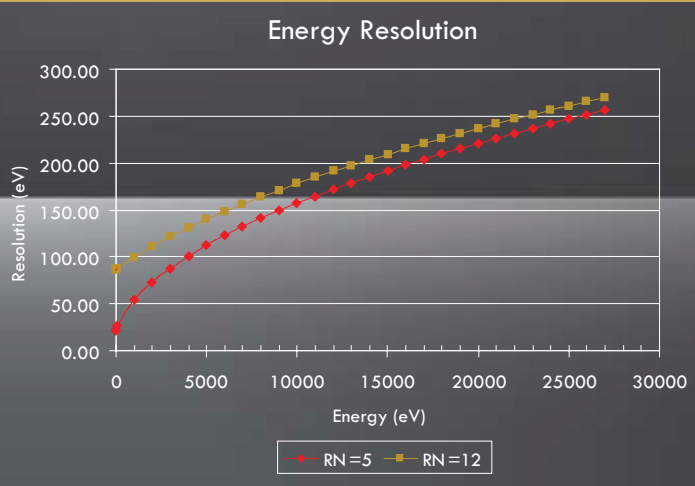

Utilizing Phosphors for Indirect Detection of X-rays

Princeton Instruments has developed two types of phosphors for x-ray imaging applications in the energy range between 5 keV and 50 keV. The GdOS:Tb is recommended for x-ray energies < 33 keV due to its higher absorption efficiency, while the CsI:Tl is recommended where higher resolution is required.

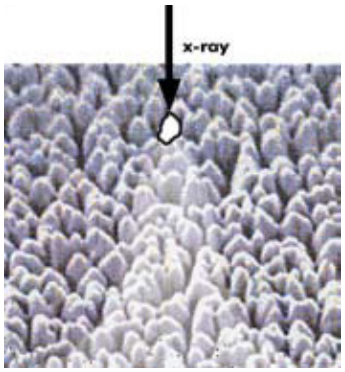

GdOS polycrystalline phosphor.

Polycrystalline Phosphor GdOS:Tb (Gadolinium Oxysulfide with Terbium)

Princeton Instruments has developed three distinct phosphors for 8, 12, and 17 keV x-ray energies based on GdOS:Tb polycrystalline powder. To provide the best possible resolution and sensitivity, small-grain powder is used on special Mylar®. These phosphors are recommended when large image area, high efficiency, and lower cost are primary considerations.

With a carefully designed experiment and a Princeton Instruments PI-SCX:1300 camera configured with a 1:1 fiberoptic, the 8 keV phosphor generates about 40 electrons for each 8 keV x-ray photon. Its FWHM resolution is about 40 to 45 µm.

When used with the same camera and a 2.5:1 fiberoptic taper, this phosphor generates about 7 electrons for each 8 keV x-ray photon. Its FWHM resolution is about 60 to 80 µm.

In similar experiments, the 17 keV phosphor generates about 65 electrons per 17 keV x-ray photon with a 1:1 fiberoptic. When used with a 2.5:1 fiberoptic taper, this phosphor generates about 10 electrons. Its FWHM resolution is also about 60 to 80 µm.

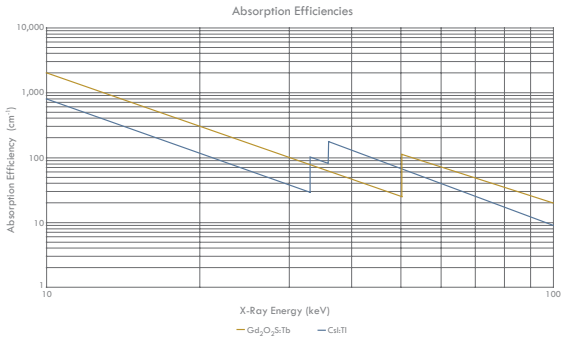

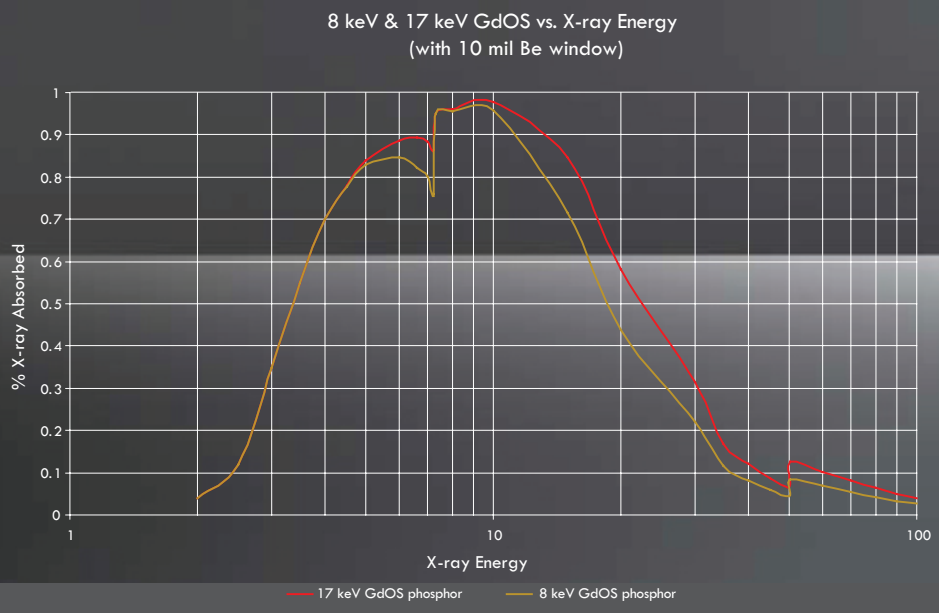

Crystalline (Needle Structure) Phosphor CsI:Tl (Cesium Iodide with Thallium)

Princeton Instruments has developed high-resolution phosphors based on crystalline (needle structure) CsI:Tl for 8 and 24 keV x-ray energies. These phosphors are recommended when high resolution is the primary consideration.

Although it has lower absorption at x-ray energies < 33 keV, the crystalline (needle structure) of CsI:Tl holds a number of advantages over GdOS:Tb powder phosphors:

- The needle structure of CsI:Tl acts as a light guide, transmitting the visible light generated by the absorbed x-ray photons.
- It provides higher resolution than polycrystalline GdOS:Tb phosphors.
- It preserves resolution when the x-ray energy changes a little from experiment-to-experiment.
- Its light output is more uniform. A special coating over the needle structure developed to preserve high resolution also protects it from moisture in the atmosphere.

With a carefully designed experiment and a Princeton Instruments PI-SCX:1300 camera configured with a 1:1 fiberoptic, the 8 keV CsI:Tl phosphor delivered FWHM resolution of < 20 µm.

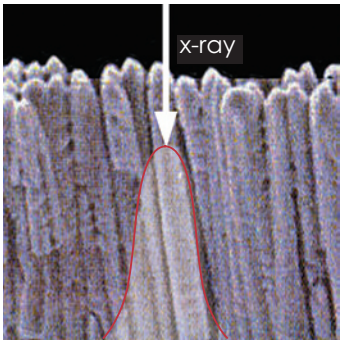

CsI:Tl needle structure.

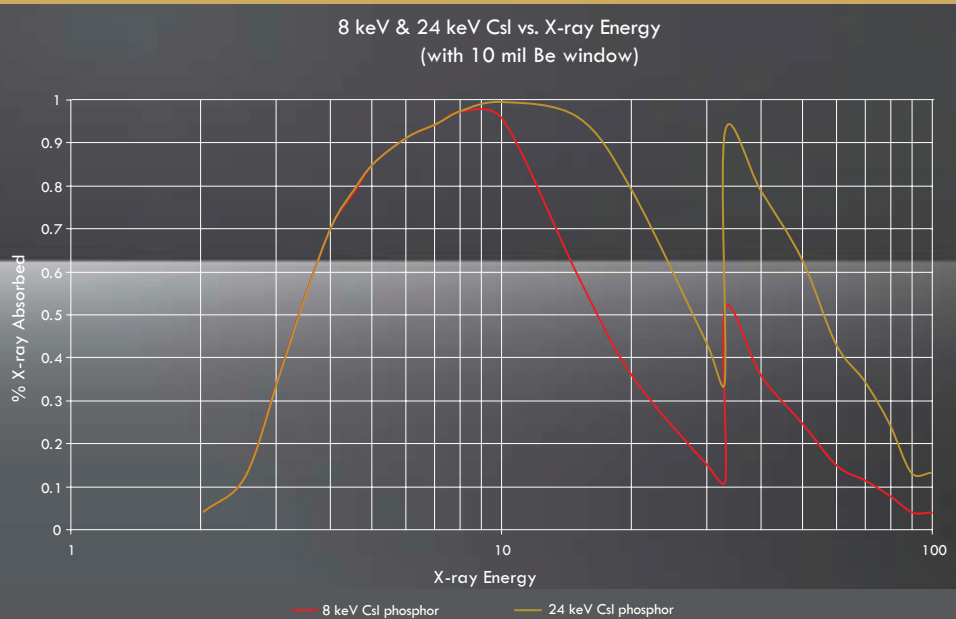

Evaluation of the Point Spread Function for a Quad-RO:4096/1/165 with an 8 keV Gd_2O_2S:Tb Phosphor

Introduction

An important performance characteristic of CCD-based imaging x-ray detectors is their ability to avoid blurring when imaging a point source. Such blurring is characterized by the point spread function (PSF) of a detector and can be expressed in terms of the full width at half maximum (FWHM) of the image (*Naday et al.,* 1994). According to *Naday et al.,* the PSF is mainly affected by the thickness of the phosphor layer and the grain size of the phosphor.

In this document we report measurements of the PSF for a Quad-RO:4096/1/165 using a Gd_2O_2S:Tb phosphor optimized for 8 keV (0.15 nm wavelength) x-ray detection.

Equipment Used

X-ray detector

- Quad-RO:4096, Grade 1 CCD, 165 mm fiberoptic (2.7:1 taper ratio), Model: 7548-0001, Serial Number: 2506080008, System ID: 94305
- Gd_2O_2S:Tb phosphor for 8 keV x-ray energy
- CCD pixel size of 15 µm (40.5 µm pixel size at the image plane)
- Thermoelectric cooling to –40 °C by circulating a 50:50 mixture of ethylene glycol and water

X-ray source

- 150 kV microfocus x-ray source, Model: L8121-03
- Focal spot size: 7 µm, 20 µm, 50 µm
- Operated at 20 kV, 250 µA

X-ray control unit

- Hamamatsu, x-ray 150 control unit

X-ray cabinet

- Security Defense Systems, Model: Inspex, Serial Number: 9906632

Miscellaneous

- Copper plate with 20 µm pinhole
- Taper-width lead cover disk

FIGURE 1.

Photo of experimental setup.

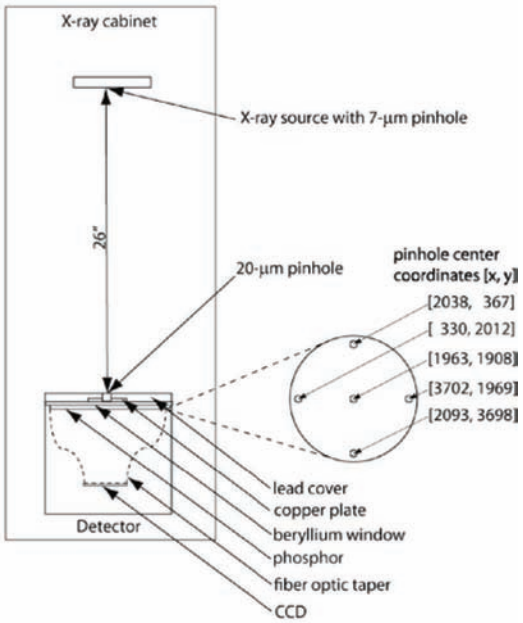

FIGURE 2.

Diagram of experimental setup.

Data Collection Procedure

Figure 2 shows key features of the experimental setup. A small copper plate with a 20 µm pinhole rests on the beryllium window above the phosphor and is covered with a lead disk. The x-ray source with a 7 µm focal spot size was 26" (66 cm) above the image plane at the beryllium window.

Five locations were selected for the copper and lead pinholes, as shown in Figure 2. The coordinates [x, y] are relative to an origin [1, 1] at the upper left corner of the sensor array.

Background subtraction and flat field normalization files were obtained and the corrections enabled before images were acquired. An exposure time of 60 sec was used for the background subtraction and pinhole image data. The exposure for the flat field file was long enough for array pixels to fill to three-quarters of the full-well capacity. Separate images were acquired for each of the five pinhole locations.

Results

Each calculated point spread function is based on a 51 × 51 region of the sensor array. Although pixel intensities can be plotted as either a function of the x- or y-coordinate on the array, Figures 3–7 show plots of intensity versus y-coordinate only as these plots show the worst possible performance due to vertical smearing. (Data is also available for the x-coordinate.)

Figures 3–7 show the point spread functions for the center, left, right, top, and bottom pinholes, respectively. Each of the PSFs obtained shows an FWHM of less than twice the image plane pixel width (40.5 µm).

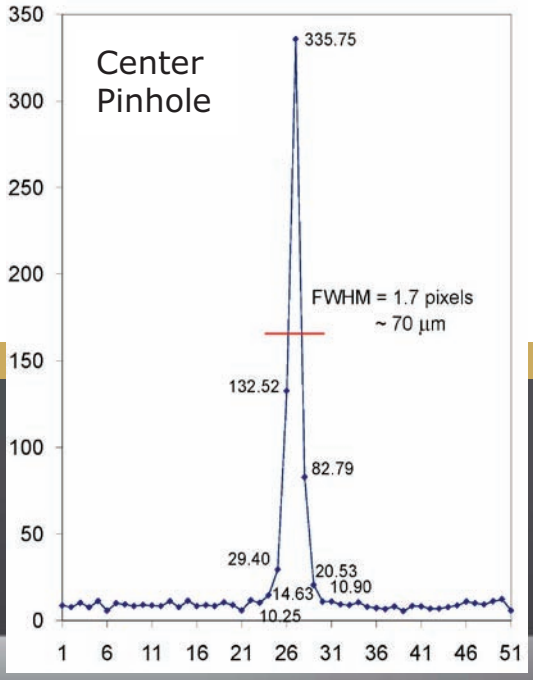

Point spread function for the center pinhole.

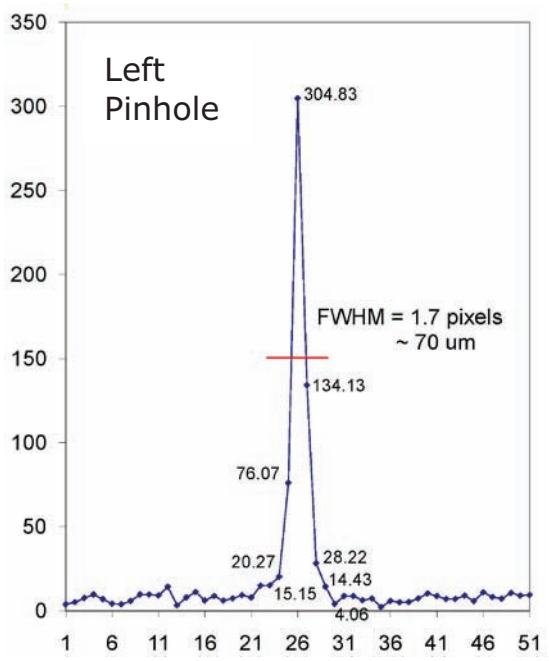

Figure 4. Point spread function for the left pinhole.

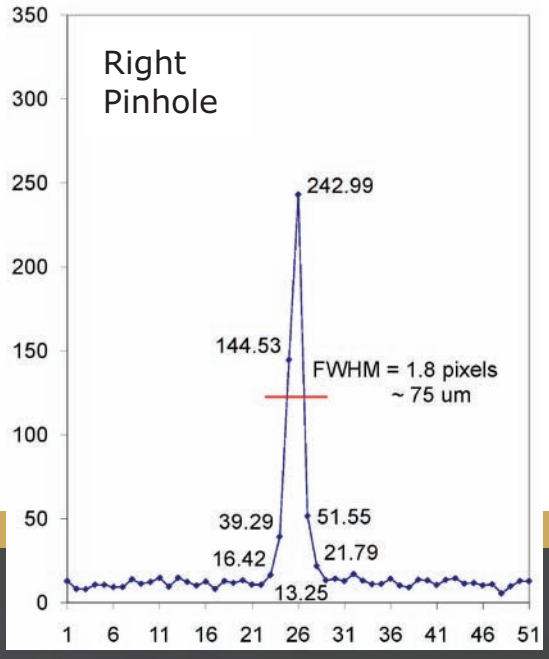

Figure 5. Point spread function for the right pinhole.

FIGURE 3.

Conclusions

The FWHM value of ~ 70 µm obtained for the center, left, top, and bottom locations with the 8 keV Gd_2O_2S:Tb phosphor demonstrates that the PSF of the Quad-RO:4096/1/165 is better than or equal to that of other commercially available detectors. This also demonstrates that the unique phosphor coupling technique used for easy replacement of the phosphor in the field does not adversely affect the PSF or degrade the performance near the sensor perimeter compared to the center and that the PSF is limited only by the pixel size at the image plane.

With the observed FWHM values less than the width of two image plane pixels, the Quad-RO:4096/1/165 will produce extremely sharp images (with negligible blurring).

References

I. Naday, S. Ross, M. Kanyo, E. Westbrook, and M. Westbrook. Characterization of CCD-based imaging X-ray detectors for diffraction experiments, *Nuclear Instruments and Methods in Physics Research A* 347, 534–538, 1994.

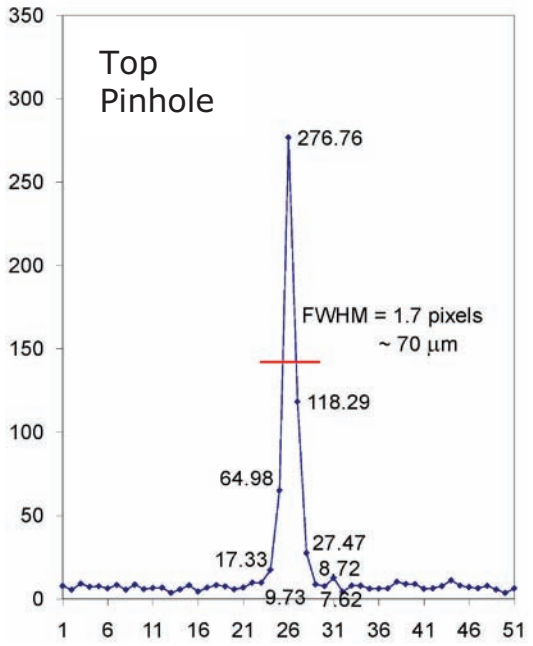

Figure 6. Point spread function for the top pinhole.

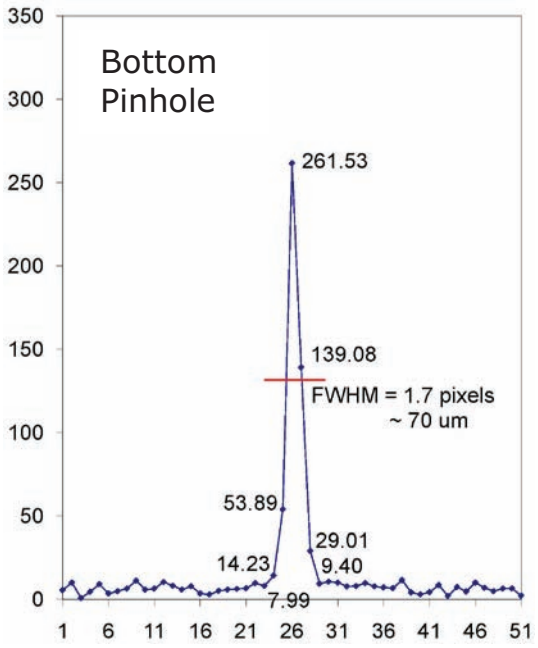

Figure 7. Point spread function for the bottom pinhole.

Evaluation of the Point Spread Function for a Quad-RO:4096/1/90 with an 8 keV Gd_2O_2S:Tb Phosphor

Introduction

An important performance characteristic of CCD-based imaging x-ray detectors is their ability to avoid blurring when imaging a point source. Such blurring is characterized by the point spread function (PSF) of a detector and can be expressed in terms of the full width at half maximum (FWHM) of the image (*Naday et al.*, 1994). According to *Naday et al.*, the PSF is mainly affected by the thickness of the phosphor layer and the grain size of the phosphor.

In this document we report measurements of the PSF for a Quad-RO:4096/1/90 using a Gd_2O_2S:Tb phosphor optimized for 8 keV (0.15 nm wavelength) x-ray detection.

Equipment Used

X-ray detector

- Quad-RO:4096, Grade 1 CCD, 90 mm fiberoptic (1:1 taper ratio), Model: 7484-0001, Serial Number: 2809070001, System ID: 91543
- Gd_2O_2S:Tb phosphor optimized for 8 keV x-ray energy
- CCD pixel size of 15 µm (15.0 µm pixel size at the image plane)
- Thermoelectric cooling to –40 °C by circulating a 50:50 mixture of ethylene glycol and water

X-ray source

- 150 kV microfocus x-ray source, Model: L8121-03
- Focal spot size: 7 µm, 20 µm, 50 µm
- Operated at 20 kV, 250 µA

X-ray control unit

- Hamamatsu, x-ray 150 control unit

X-ray cabinet

- Security Defense Systems, Model: Inspex, Serial Number: 9906632

Miscellaneous

- 5 µm pinhole
- Lead cover disk

FIGURE 1.

Photo of experimental setup.

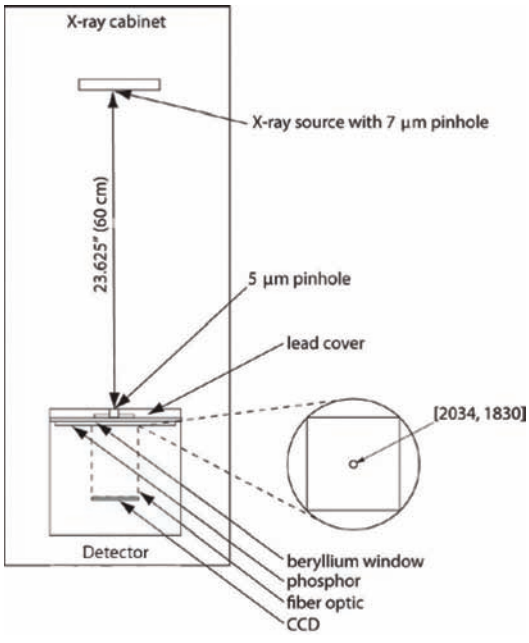

FIGURE 2.

Diagram of experimental setup.

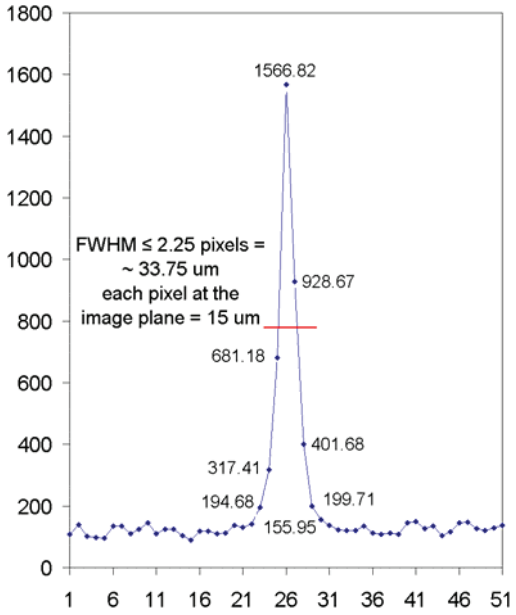

Figure 3. Y direction point spread function for the center pinhole.

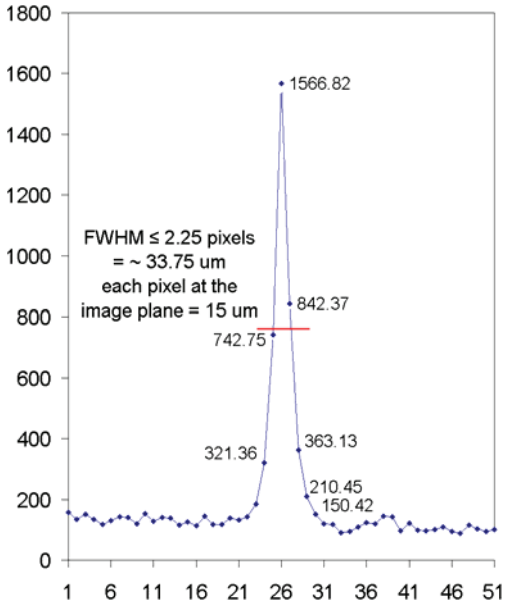

Figure 4. X direction point spread function for the center pinhole.

Data Collection Procedure

Figure 2 shows key features of the experimental setup. A small 5 µm pinhole rests on the beryllium window above the phosphor and is covered with a lead disk. The x-ray source with a 7 µm focal spot size was 23.625" (60 cm) above the image plane at the beryllium window.

Since the detector has a 1:1 fiberoptic faceplate, only one center location was used.

Background subtraction and flat field normalization files were obtained and the corrections enabled before images were acquired. An exposure time of 300 sec was used for the background subtraction and pinhole image data. The exposure for the flat field file was long enough for array pixels to fill to three-quarters of the full-well capacity.

Results

The calculated point spread function is based on a 51 × 51 region of the sensor array. Figure 3 shows the y-coordinate point spread function for the center pinhole. The PSF obtained shows an FWHM of ~ 33.75 µm. Data for the x-coordinate is shown in Figure 4. Figure 5 shows a three-dimensional representation.

Conclusions

The FWHM value of ~ 33.75 µm obtained for the center location with the 8 keV Gd_2O_2S:Tb phosphor demonstrates that the PSF of the Quad-RO:4096/1/90 is better than any other commercially available detector. This also demonstrates that the unique phosphor coupling technique used for easy replacement of the phosphor in the field does not adversely affect the PSF.

With the observed FWHM value of ~ 33.75 µm, the Quad-RO:4096/1/90 will produce extremely sharp images (with negligible blurring).

References

I. Naday, S. Ross, M. Kanyo, E. Westbrook, and M. Westbrook. Characterization of CCD-based imaging X-ray detectors for diffraction experiments, *Nuclear Instruments and Methods in Physics Research A* 347, 534–538, 1994.

FIGURE 5.

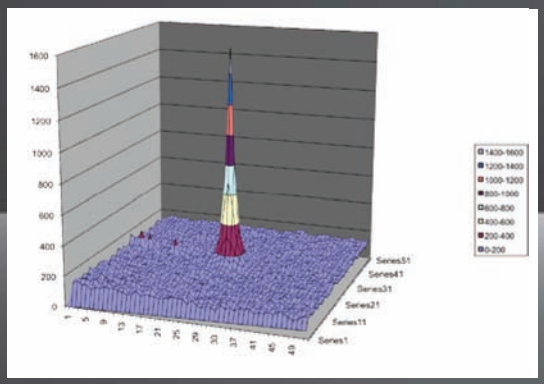

3D plot of the center pinhole.

Evaluation of the Point Spread Function for a PIXIS-XF:2048F with a 17 keV Gd_2O_2S:Tb Phosphor

Introduction

An important performance characteristic of CCD-based imaging x-ray detectors is their ability to avoid blurring when imaging a point source. Such blurring is characterized by the point spread function (PSF) of a detector and can be expressed in terms of the full width at half maximum (FWHM) of the image (*Naday et al.*, 1994). According to *Naday et al.*, the PSF is mainly affected by the thickness of the phosphor layer and the grain size of the phosphor.

In this document we report measurements of the PSF for a PIXIS-XF:2048F using a Gd_2O_2S:Tb phosphor optimized for 17 keV (0.073 nm wavelength) x-ray detection.

Equipment Used

X-ray detector

- PIXIS-XF:2048F, Grade 1 CCD, 40 mm fiberoptic (1:1 taper ratio), Model: 7538-0009, Serial Number: 1811080009, System ID: 93186
- Gd_2O_2S:Tb phosphor optimized for 17 keV x-ray energy
- CCD pixel size of 13.5 µm (13.5 µm pixel size at the image plane)
- Thermoelectric cooling to –30 °C by air

X-ray source

- 150 kV microfocus x-ray source, Model: L8121-03
- Focal spot size: 7 µm, 20 µm, 50 µm
- Operated at 35 kV, 250 µA

X-ray control unit

- Hamamatsu, x-ray 150 control unit

X-ray cabinet

- Security Defense Systems, Model: Inspex, Serial Number: 9906632

Miscellaneous

- 5 µm pinhole
- Lead cover disk

FIGURE 1.

Photo of experimental setup.

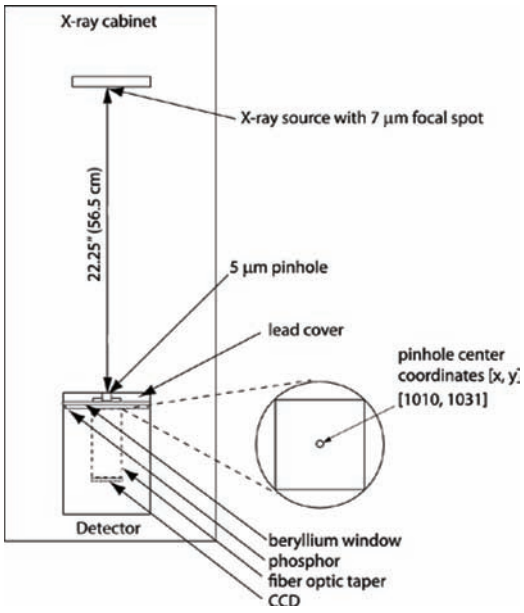

FIGURE 2.

Diagram of experimental setup.

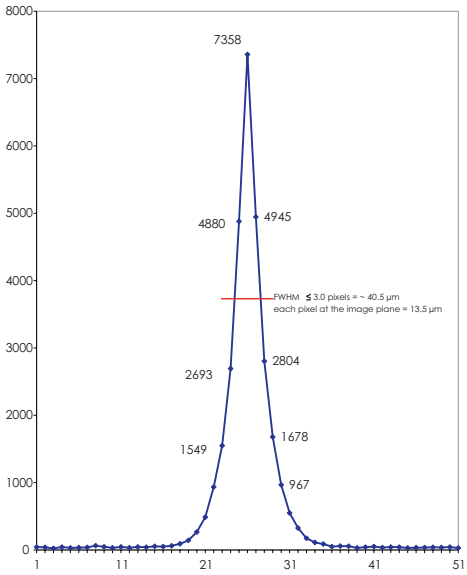

Figure 3. Y direction point spread function for the center pinhole.

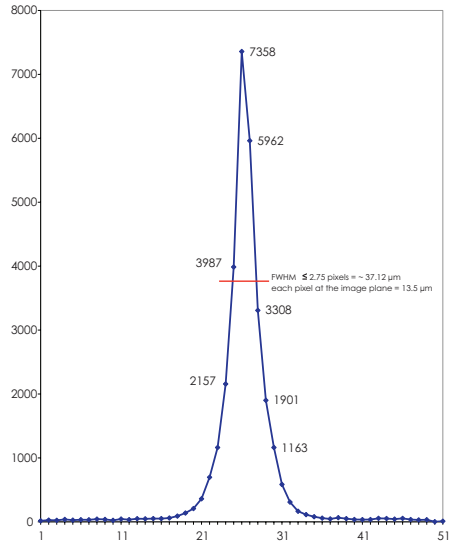

Figure 4. X direction point spread function for the center pinhole.

Data Collection Procedure

Figure 2 shows key features of the experimental setup. A small 5 µm pinhole rests on the beryllium window above the phosphor and is covered with a lead disk. The x-ray source with a 7 µm focal spot size was 22.25" (56.5 cm) above the image plane at the beryllium window.

Since the detector has a 1:1 fiberoptic faceplate, only one center location was used.

Background subtraction and flat field normalization files were obtained and the corrections enabled before images were acquired. An exposure time of 250 sec was used for the background subtraction and pinhole image data. The exposure for the flat field file was long enough for array pixels to fill to three-quarters of the full-well capacity.

Results

The calculated point spread function is based on a 51 × 51 region of the sensor array. Figure 3 shows the y-coordinate point spread function for the center pinhole. The PSF obtained shows an FWHM of ~ 40.5 µm.

Data for the x-coordinate is shown in Figure 4.

Figure 5 shows a three-dimensional representation.

Conclusions

The FWHM value of ~ 40.5 µm obtained for the center location with the 17 keV Gd_2O_2S:Tb phosphor demonstrates that the PSF of the PIXIS-XF:2048F is better than any other commercially available detector. This also demonstrates that the unique phosphor coupling technique used for easy replacement of the phosphor in the field does not adversely affect the PSF.

With the observed FWHM value of ~ 40.5 µm, the PIXIS-XF:2048F will produce extremely sharp images (with negligible blurring).

References

I. Naday, S. Ross, M. Kanyo, E. Westbrook, and M. Westbrook. Characterization of CCD-based imaging X-ray detectors for diffraction experiments, *Nuclear Instruments and Methods in Physics Research* A 347, 534–538, 1994.

FIGURE 5.

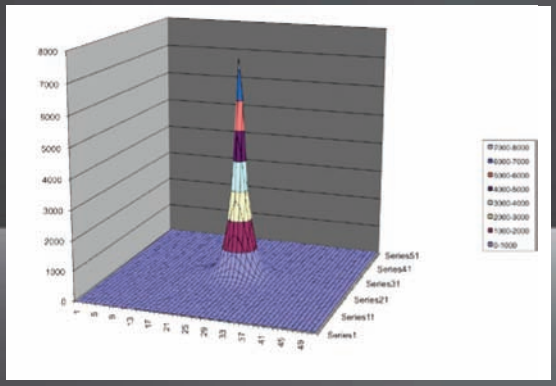

3D plot of the center pinhole.

Use of Fiberoptics for Indirect Detection of X-rays

Quite often, users of indirect-detection systems assume that the CCD camera manufacturer has carefully selected a proper combination of CCD + fiberoptic (faceplate or taper) + phosphor to preserve image quality. Unfortunately, it is difficult for a manufacturer to know the requirements for every application. Therefore, it is particularly important that each customer understands the options available for one of the more vital components of the system (i.e., the fiberoptic faceplate or taper) and makes a selection that best meets performance requirements. Such requirements include the best possible transmission efficiency, contrast, and sensitivity, as well as the lowest acceptable distortion, the best possible CCD, and the lowest-noise / highest-speed electronics.

Years ago, it was easy to select a fiberoptic. There were only one or two options available. As fiberoptic manufacturers developed new technologies, however, it became very important that customers be aware of the available options. The main specifications to consider when selecting a fiberoptic are (1) the size of the fibers in the fiberoptic, (2) the type of extramural absorber (EMA), and (3) blemishes and distortions.

Size of Fibers in a Fiberoptic

When coupling a fiberoptic to a CCD, the ideal size of the fiber will be the same as the CCD pixel size. Unfortunately, it is practically impossible to manufacture a fiberoptic faceplate or taper with a fiber pattern/size that will precisely match the pixel pattern (Figure 1). However, if the fiber size is selected to best match the pixel size, a mismatch will occur (Figure 2) and a huge variation in pixel-to-pixel sensitivity (pixel-to-pixel response nonuniformity) will occur, which will be undesirable for almost all applications.

To avoid this situation, it is very important to choose a fiber size that is significantly (but practically) smaller than the CCD pixel size, so there are many fibers per pixel. For this reason, Princeton Instruments camera systems utilize a fiber size that is 3–4 times smaller than the CCD pixel size (or as small as practically possible), so there are at least 9 fibers per pixel (Figure 3) to preserve the best image quality.

Type of Extramural Absorber (EMA)

Once the fiber size is selected in a fiberoptic faceplate or taper to absorb scattered light in the fiberoptic, it is very important to choose the right type of EMA. There are a few different types of EMAs available, each with its own advantages and disadvantages, each with different variations added from time-to-time to enhance performance.

(a) Interstitial EMA

In interstitial EMA types (Figures 4 and 5), small black fibers are strategically placed between the fiberoptic stitching boundaries. The uniform distribution of the EMA fibers in this design ensures that most of the stray light is absorbed before reaching the output surface.

Note: The interstitial EMA shown in Figure 4 is the primary type used by Schott Inc.

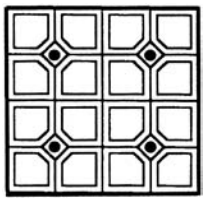

Figure 4

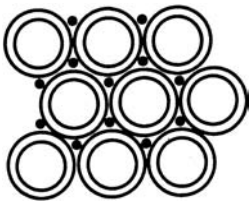

Figure 5

FIGURE 1.

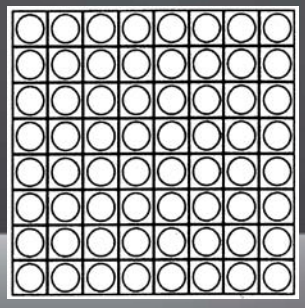

Ideal fiber-to-pixel arrangement.

FIGURE 2.

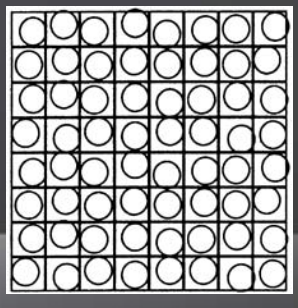

Realistic fiber coupling.

(b) Statistical EMA

In statistical EMA types (Figure 6), black EMA fibers of the same diameter as the optical fibers are inserted at strategic locations while assembling the multi-assembly. Due to the positioning of EMA fibers in this type, the MTF and resolution performance of this EMA is somewhat inferior to the interstitial EMA. The statistical nature of this EMA allows the manufacturer to control the percentage of EMA used to deliver the highest possible transmission efficiency. To deliver acceptable performance in most applications, manufacturers use about 6% black fibers.

Note: The statistical EMA shown in Figure 6 is the preferred type used by INCOM. Owing to its exceptional performance and flexibility, Princeton Instruments utilizes statistical EMA in the majority of our indirect-detection CCD camera systems.

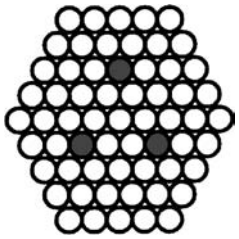

Figure 6

(c) Annular EMA

In the annular EMA type (Figure 7), each monofiber is surrounded by a thin black cladding. This annular EMA construction ensures the most uniform EMA distribution within the fiberoptic structure and results in very high MTF and resolution. Manufacturing fiberoptics with annular EMA is more expensive due to the need for highly absorbent black glass and thermal properties that facilitate high yield when fusing with standard fibers. These fibers have the lowest transmission efficiency and therefore are used in very special applications only.

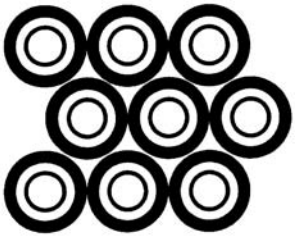

Figure 7

(d) Enhanced EMA

In the enhanced EMA type (Figure 8), an improved statistical EMA design is utilized with higher light absorbing dark fibers than those in the standard statistical EMA design, thus delivering a better-contrast image. Since the relatively recent introduction of this type of EMA (by INCOM), only fiberoptic faceplates (1:1) are available.

Note: For special high-contrast applications, Princeton Instruments uses enhanced EMA (1:1 faceplate, typically with 6 µm fiber size).

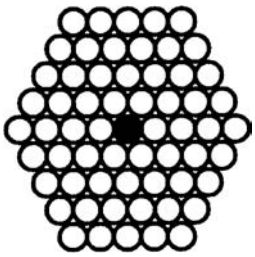

Figure 8

FIGURE 3.

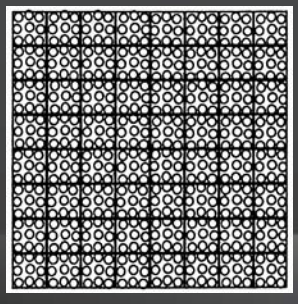

Good fiber-to-pixel arrangement.

Blemishes and Distortions

When fusing single (mono) fibers to build multi-fibers, or when fusing multi-fibers to build multi-multi fibers (to build a large boule) to manufacture a fiberoptic faceplate or taper, some defects are introduced. It is very important to know about these defects, as they degrade the quality of the image. There are two major types of defects: blemishes and distortions.

(a) Blemishes

There are two types of blemishes: spot blemishes and line blemishes.

Spot blemishes, groups of non-transmitting fibers, are caused by contaminants that are trapped between fibers during drawing operations and are left behind after fibers are cleaned and fused. The trapped contaminants are not reduced in size during the drawing operations and eventually impact one or more fibers causing light to scatter, resulting in non-transmitting fibers.

Line blemishes are chicken-wire patterns at the multi-multi boundaries that are caused by damage to the fibers at the outside edges of multi-multis when they are improperly cleaned. Line blemishes can also occur due to improper temperature or pressure control in the pressing operation.

(b) Distortions

There are two types of distortions: shear distortions and gross distortions.

Shear distortions are caused by misalignment of multi-multi fibers along the length of a fusion. They are the lateral displacements that cause a straight line to be imaged as a "break". This results in a small break in the coherency of the image in the final component. They are extremely difficult to correct.

Gross distortions are caused by material flow in the fusing operation. They are defined as distortions that cause a straight line to be imaged as a continuous curve. Proper control of temperature and pressure during pressing can minimize this kind of distortion, which is defined as the maximum displacement from a straight line. Improvements in the manufacturing process over the years have reduced this type of distortion to less than 2% of the clear aperture of the final component for boule sizes up to 165 mm in diameter.

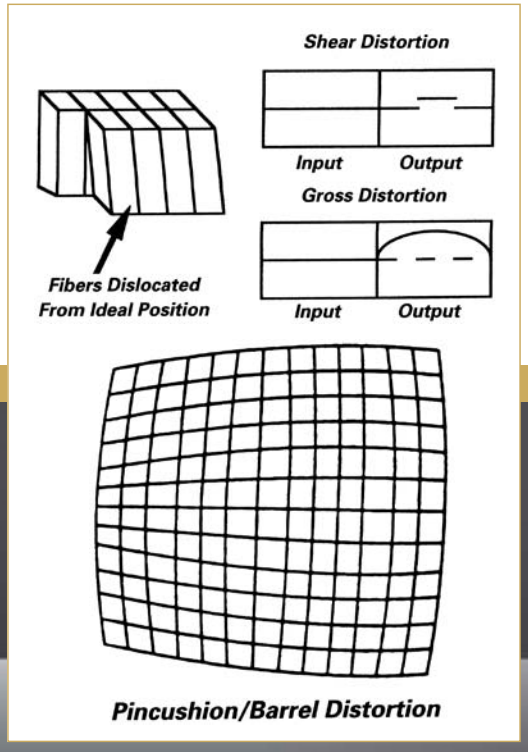

APPLICATION BRIEFS

Direct-Detection Applications

EUV Lithography
Next-Generation Technology for the Semiconductor Industry

Dr. Gordon Moore, co-founder of Intel Corp., described the progress of the development of semiconductor devices with a sentence that is now commonly known as Moore's Law: The number of transistors on a computer chip doubles every 1.5 to 2 years.

Moore's Law is not only a description of the evolution of semiconductors, but has also served as a roadmap for chip manufacturers and the suppliers of chip production tools. In semiconductor chip production, lithography is a critical manufacturing method used to ensure both sufficient quality and high throughput. Optical lithography remains the traditional technique used in the semiconductor industry. The lithography chip manufacturing process can be defined as follows:

- Light (any wavelength) from the source passes through optics to generate homogenous illumination of the mask.
- The mask image is projected on the photoresist-coated wafer using another set of optics with certain demagnification to produce fine structures.
- The illuminated areas from the wafer are removed using a chemical process.
- This is followed by etching or coating uncovered parts.
- This process is repeated over and over to produce current super complex chips.

The semiconductor industry uses a light source with wavelengths from 365 nm to 248 nm to 193 / 157 nm and produces feature sizes < 100 nm, but it has reached the technological limit of optical lithography. Recognizing this limitation, the industry has spent the past several years identifying a potential successor technology to produce features < 100 nm. Next-generation lithography technologies investigated by the semiconductor industry include EUV lithography, x-ray lithography, ion-beam projection lithography, and electron-beam projection lithography.

Although EUV lithography has its share of challenges, it is often used because it (1) retains the look and feel of the current optical lithography process (wavelength: 13.5 nm) described above and (2) uses the same basic design tools.

Since this wavelength (13.5 nm, or ~ 92 eV) is absorbed in the air and requires a high vacuum for transmission, it places extreme challenges on all parts of production tools. First of all, the light source has to deliver a narrow band of high-EUV power (preferably with high spectral purity) in order to guarantee high throughput. Second, all components that move the mask and the wafer with nanometer precision need to be operated in ultra-high-vacuum environments. Third, projection optics need to deliver dynamic positioning precision in the Angstrom range and be contamination-free down to the level of a few nanometers in order to deliver high efficiency.

To keep all these components in good working condition and delivering the highest performance possible, the best diagnostics and monitoring tools are required. Among the tools that have served the EUV research community well for diagnostics and monitoring of the EUV light source are soft x-ray imaging systems from Princeton Instruments.

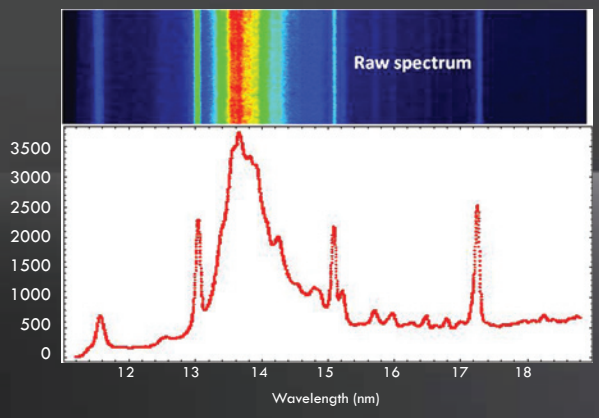

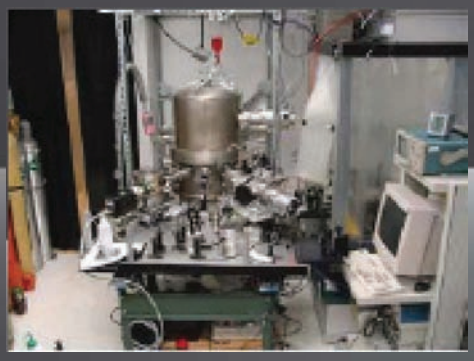

Photo courtesy of Professor Martin Richardson, Laser Plasma Laboratory, Center for Research and Education in Optics and Lasers (CREOL), University of Central Florida.

Soft X-ray Microscopy

Soft x-ray microscopy is used for imaging and researching the elemental composition and structure of biological, materials science, and other samples. With a wavelength range between 4.0 Angstroms (~ 3.0 keV) and 44 Angstroms (~ 300 eV), these microscopes are capable of achieving spatial resolution of several hundreds of Angstroms, about 10x better resolution than the maximum of visible light microscopes.

The primary advantages of a soft x-ray microscope are its design simplicity and its ability to form high-spatial-resolution images of thick, hydrated biological samples in a near-native environment without the time-consuming preparation required by electron microscopes. Since biological samples consist largely of hydrogen, carbon, oxygen, and nitrogen (with additional amounts of seven other elements and important trace elements), and have their primary absorption edges (except hydrogen) in the water window between the absorption edge of carbon (284 eV, 4.4 nm) and oxygen (543 eV, 2.3 nm), the soft x-ray microscope provides excellent spectroscopic information and delivers high-contrast images.

In a soft x-ray microscope arrangement, soft x-rays from a synchrotron are guided along a beamline and the sample is exposed. A zone plate lens is used to form an image of the transmitted x-rays onto a scientific CCD detector and a high-contrast image is captured.

In a scanning soft x-ray microscope arrangement, monochromatic soft x-rays from a synchrotron are guided along a beamline and impinge on the zone plate, which focuses the x-rays very sharply on a single point (diameter: < 0.1 µm) on the sample. The sample is scanned and information regarding absorption versus position is recorded. This step is repeated several times with different monochromatic x-rays and an image is constructed pixel-by-pixel in the software. The scanning method provides excellent elemental and chemical analyses at very high spectral resolutions, limited only by synchrotron instrumentation.

Soft X-ray Plasma Diagnostics

Hot and dense plasmas are of enormous interest in basic physics research because of the multitude of compelling phenomena which arise from them. Moreover, they are of much technological and industrial importance in research areas such as laser fusion, EUV, soft x-ray lasers, and lithography, as well as many other areas known for concentrated energy densities. Because of their high energy concentration, these plasmas tend to involve rapid expansions, thus sharpening gradients in density and other parameters. As hot and dense plasmas become fully ionized, the radiation starts to consist of a broad continuum of bremsstrahlung due to free electron-ion interactions and narrow-line emissions caused by bound-bound transitions in the atoms (ions) of various charge states.

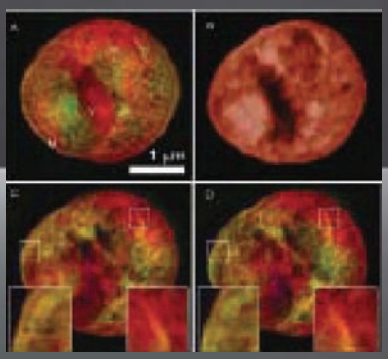

Image courtesy of Prof. Chris Jacobsen et al., Department of Physics and Astronomy, Stony Brook University, NY.

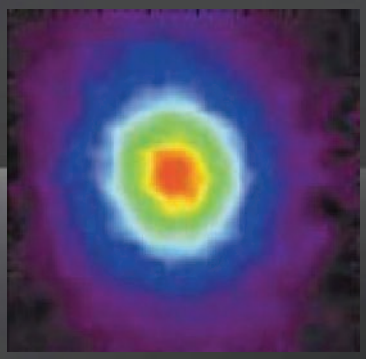

Indirect-Detection Applications

X-ray Diffraction

X-ray diffraction is a technique for studying the characteristics of matter such as macromolecules, crystals, powders, polymers, and fibers. When x-rays pass through matter they interact with electrons in the atoms and become scattered. If the atoms are organized in planes (i.e., the matter is crystalline) and the distances between the atoms are of the same magnitude as the wavelength of the x-rays, then constructive and destructive interference occurs and a diffraction pattern forms. Different types of x-rays (e.g., monochromatic, pink beam, or white beam) are utilized to study a wide variety of matter.

X-ray Crystallography

The theory of crystallography was developed soon after x-rays were first discovered by W. C. Roentgen in 1895. Since then, the theory has undergone continual development ushered along by advances in data collection instrumentation and data reduction methods. In recent years, the advent of synchrotron radiation sources, microfocus x-ray tubes, high-efficiency optics, area detector-based data collection instruments, and high-speed computers has dramatically enhanced the efficiency of crystallographic structural determination. For crystal structure determination, integrated intensities of the diffraction peaks (as shown in the image below) are created using monochromatic x-rays and then used to reconstruct the electron density map within the unit cell in the crystal.

To attain high accuracy in the reconstruction, which is created by Fourier transforming the diffraction intensities with the appropriate phase assignment, a high degree of completeness and redundancy in the diffraction data is necessary. In other words, all possible reflections are measured multiple times in order to reduce systematic and statistical errors.

The most efficient way to achieve this is to use a CCD detector, which can collect diffraction data in a large, solid angle. Today, x-ray crystallography is widely used in materials science and biological research. Structures of very large biological machinery (e.g., protein and DNA complexes, virus particles) have been determined using this method.

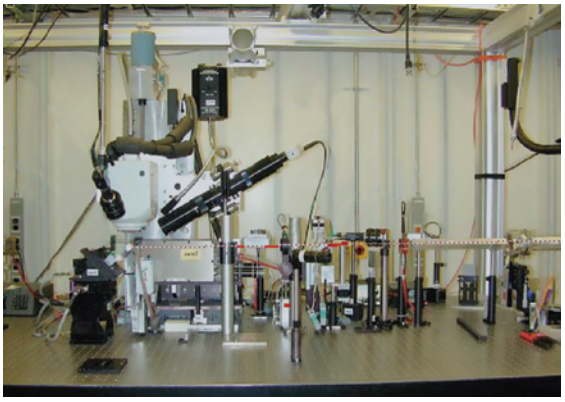

Photo courtesy of Dr. Gene Ice, Oak Ridge National Laboratory (ORNL), Oak Ridge, TN 37830, USA. UNICAT 34-ID-E X-ray Micro-Diffraction Facility.

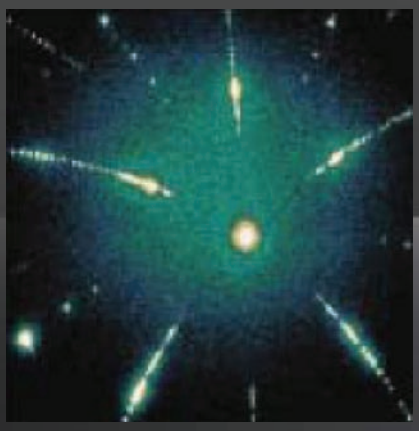

A microLaue pattern from a pendeoepitaxial film of GaN grown on single-crystal SiC. Image courtesy of Dr. Gene Ice, Oak Ridge National Laboratory (ORNL), Oak Ridge, TN, USA.

Image courtesy of S.M. Polvino and H. Yan, Department of Applied Physics and Applied Math, Columbia University, New York, NY.

APPLICATION NOTES

www.princetoninstruments.com

X-ray Phase-Contrast Imaging

Introduction

As the selection of high-sensitivity scientific detectors, custom phosphor screens, and advanced x-ray sources available to researchers continues to expand, so too does the scope and variety of x-ray phase-contrast imaging techniques. This note describes a new application of phase-contrast imaging in which high-performance Princeton Instruments Quad-RO and PI-SCX cameras are utilized to acquire high-resolution, quantitative x-ray images.

X-ray Phase-Contrast Imaging

X-ray phase-contrast imaging is an important method for visualizing cellular and histological structures for a wide range of biological and medical studies. While traditional x-ray imaging yields an image that maps a sample's absorptive properties by measuring x-ray photon flux from an x-ray source after it traverses a sample, x-ray phase-contrast imaging uses a spatially coherent beam and a high-resolution detector to acquire a clearer, more detailed image of the sample. As the beam's coherent x-ray photons traverse regions of differing indices of x-ray refraction in a sample, they are refracted and undergo a phase shift, thereby losing coherence and creating constructive and destructive interference patterns with unrefracted photons (see Figure 1). These patterns enable high-contrast imaging of interfaces within the sample.[1]

System Description

Recently, the groups of Dr. Christoph Rose-Petruck and Dr. Gerald Diebold at Brown University and researchers from the Liver Research Center, Rhode Island Hospital and Warren Alpert Medical School of Brown University, developed an experiment protocol in which a microfocus x-ray source and a scientific detector are used to produce high-resolution, phase-contrast images of vasculature in fixed mouse livers. Their collaboration with colleagues at the Illinois Institute of Technology subsequently expanded this work to phase-contrast, computed tomographic imaging of fixed murine livers.[1] This Princeton Instruments application note briefly details their imaging system setup and presents some of the data acquired.

X-ray Source

A microfocus x-ray source is used to accelerate electrons to 90 keV at a focused point on a tungsten anode 20 µm in diameter. The deceleration of the electrons as they interact with the anode produces polychromatic x-radiation emitted from the 20 µm electron beam focus. The focus size is the limit of the resolution and spatial coherence. Typically, R1 is ~ 60 cm, R2 is ~ 180 cm, and the magnification is ~ 3x (see Figure 2).

Detector

To reduce x-ray absorption in air, the x-ray beam traverses a helium environment and impinges on a GdOS:Tb phosphor-coupled CCD. The CCD camera is a thermoelectrically cooled, 16 megapixel Princeton Instruments PI-SCX with 15 µm pixels arranged in a 4096 x 4096 array.

FIGURE 1.

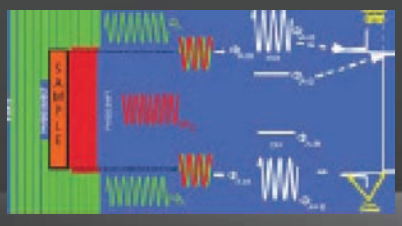

Phase interference effects at edges of the phase object enhance absorption contrast.

FIGURE 2.

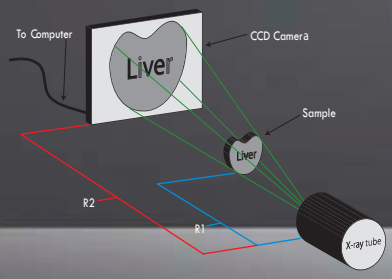

X-ray phase-contrast imaging system setup. Diagram courtesy of Dr. Christoph Rose-Petruck, Department of Chemistry, Brown University.

Protocol and Results

Excised samples are immersed in formaldehyde, which cross-links the proteins in the liver. Then the samples are dehumidified by less than 20% to allow the vessels and microvessels to fill with air. The density gradient at the air/soft-tissue interface generates strong x-ray absorption and phase-contrast features.

The resultant vascular images are resolved down to the 20 µm scale (see Figure 3), encompassing the size of the smallest vessels. Other images, taken with water-filled vessels, exhibit the same resolution but require longer exposure times.

By employing a murine model of human colon cancer metastasized into the liver, early-stage tumors and associated vascularization can be observed via this imaging scheme.[1] Vascular growth and necrosis play a key role in the proliferation dynamics of several human pathologies, explain the researchers. Many types of carcinomas signal neovascularization from nearby blood vessels, giving the tumor access to nutrients essential for growth and metastasis. Therefore, the researchers note, vascular imaging is of critical importance for studying vascular growth dynamics and potentially determining the efficacy of therapeutic drugs aimed at preventing neovascularization.

Future Applications

In addition to the PI-SCX camera referenced in this experiment protocol, the Rose-Petruck/Diebold Imaging Group now utilizes a Princeton Instruments Quad-RO camera. Like the PI-SCX, the Quad-RO features a thermoelectrically cooled CCD to deliver good quantum efficiency (QE) at 550 nm. Also like its PI-SCX predecessor, the Quad-RO can be configured with a high-resolution photosensitive array of 4096 x 4096 pixels, each measuring 15 µm, that affords a full 61 mm x 61 mm field of view.

The Quad-RO, however, offers researchers several new performance advantages. Perhaps most significantly, while the PI-SCX provides single-port readout, the Quad-RO boasts four-port readout. Electronically balanced quadrants, matched within 1.0%, yield extremely uniform raw images. Dr. Rose-Petruck reports a readout time of ~ 4 sec per full-resolution image with the Quad-RO, as opposed to ~ 17 sec per full-resolution image with the PI-SCX.

He goes on to indicate that a likely next step in his laboratory will be the development of a similar protocol for *ex vivo* perfusion imaging of livers. Another potential application involves the simultaneous use of ultrasound (structural differences in tissue are characterized by acoustic differences) to further enhance the x-ray image contrast. Highly advanced scientific detectors such as the Quad-RO x-ray camera can help facilitate progress in emerging research areas such as these.

FIGURE 3.

Data acquired with a Princeton Instruments PI-SCX:4096 camera using x-ray phase-contrast imaging. Image courtesy of Dr. Christoph Rose-Petruck, Department of Chemistry, Brown University.

Quad-RO

Designed for indirect imaging of x-rays or other Lambertian sources, the Princeton Instruments Quad-RO camera (see Figure 4) not only offers the ability to read out at four ports, it provides two readout speeds per port, on-board memory for loss-free images, and an industry-standard FireWire (IEEE 1394a) interface.

Figure 4. Multiple-port Princeton Instruments Quad-RO camera.

Software-selectable, dual-speed operation (500 kHz or 1 MHz) and multiple gain settings allow researchers to tailor Quad-RO imaging performance for practically any demanding medium-energy (3.5 keV to 150 keV) x-ray application.

Phosphor Screens

The Quad-RO camera's industry-unique mechanical design, in which the fiberoptic extends outside the vacuum, offers the flexibility needed to optimize system performance at the desired x-ray energy *in the lab* with custom phosphor screens.

GdOS:Tb phosphor screens are available for 8, 12, and 17 keV at an emission wavelength of 550 nm. CsI:Tl phosphor screens are also offered.

REFERENCES

1. "High-resolution angiography: Computed tomography coupled X-ray phase contrast imaging of excised murine liver samples," C. M. Laperle[a], P. Wintermeyer[b], E. Walker[a], D. Shi[c], M. Anastasio[c], C. Rose-Petruck[a], G. Diebold[a], and J. R. Wands[b], *Physics in Medicine and Biology* **53**, 6911-6923 (2008).

[a] Department of Chemistry, Brown University
[b] The Liver Research Center, Rhode Island Hospital and Warren Alpert Medical School of Brown University
[c] Department of Biomedical Engineering, Illinois Institute of Technology, Chicago, Illinois 60616

RESOURCES

For more information about high-performance x-ray cameras from Princeton Instruments, please visit: **www.princetoninstruments.com**

For more information about Dr. Rose-Petruck's research, please visit: **www.rosepetruck.chem.brown.edu**

Coherent X-ray Diffraction Imaging

Introduction

The use of coherent x-ray diffraction imaging is growing rapidly, facilitating numerous discoveries in the realms of biology and nanoscience as well as driving the need for high-brilliance x-ray sources. This note discusses the role of Princeton Instruments PI-LCX and PIXIS-XO cameras in such research.

Coherent X-ray Diffraction Imaging

In coherent x-ray diffraction imaging, a scientific-grade CCD camera is used to detect the continuous diffraction pattern that results from shining a pink x-ray beam on a noncrystalline specimen (see Figure 1).

Dr. Jianwei Miao, an associate professor in the Department of Physics and Astronomy and the California NanoSystems Institute at UCLA, explains that unlike microscopy techniques, which utilize physical lenses, coherent x-ray diffraction imaging is a lensless method that is wholly reliant on the use of a high-brilliance x-ray source (e.g., a third-generation synchrotron) and advanced computation.

Exposure times from 0.1 to 0.2 seconds are typical for collection of low-resolution intensity data; high-resolution intensity data requires the accumulation of tens or hundreds of frames with exposure times up to a few minutes each in order to ensure wide dynamic range. An algorithm is then applied to reconstruct 2D or 3D images from the quantitative data set acquired. Direct phase recovery is achieved via oversampling.

Post-processing times vary. A single day may be sufficient to create relatively basic 2D images, while more detailed images can take 3 days. As many as 10 days may be needed to produce high-resolution images with extensive 3D information.

Application-Specific Requirements

In 1999, Dr. Miao became the first researcher in the world to employ coherent x-rays to image noncrystalline specimens in an experimental demonstration.[1] Over the course of the past decade, he has used coherent x-ray diffraction imaging to perform studies involving organic as well as inorganic samples (see Figure 2).

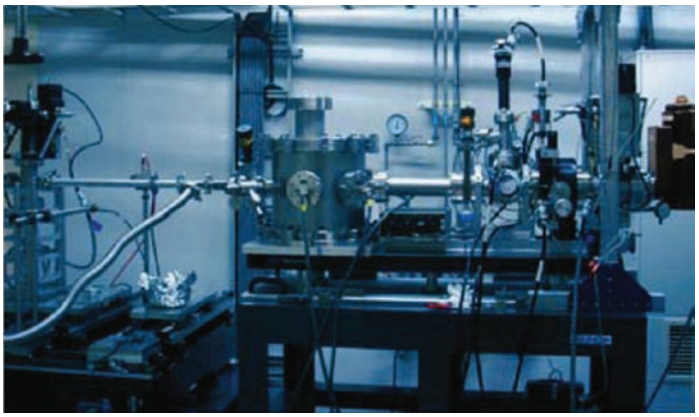

Figure 2. An experimental setup for coherent x-ray diffraction imaging at SPring-8, Japan, currently the most powerful x-ray source in the world. Photo courtesy of Dr. Jianwei Miao, University of California, Los Angeles.

FIGURE 1.

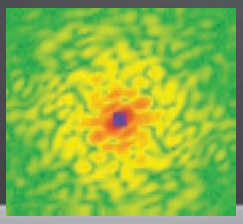

Unprocessed, far-field diffraction pattern acquired during coherent x-ray diffraction imaging experiment. Data courtesy of Dr. Jianwei Miao, University of California, Los Angeles.

Dr. Miao has relied on advanced x-ray imaging instrumentation from Princeton Instruments since 1996, utilizing several PI-LCX and PI-SX (now known as PIXIS-XO) cameras in his work. Key detection technology criteria for coherent x-ray diffraction imaging include wide dynamic range, high sensitivity, high quantum efficiency, and an array comprising many pixels. Fast readout is also important, as samples are commonly probed by an x-ray beam at rates up to 120 pulses/sec (120 Hz) in these experiments.

The characteristics of the specimen itself dictate the x-ray energy to be used.[2-9] One research area in which coherent x-ray diffraction imaging is proving to be highly valuable is nanoscience, especially the investigation of nanomaterials and nanostructure (see Figure 3).

When imaging nanoparticles, hard x-rays in the 5 keV to 7 keV range are typically employed to achieve high resolution. Dr. Miao utilizes an LN_2-cooled PI-LCX with a 1340 x 1300 array to detect the nanoparticle's diffraction patterns, owing to the camera's excellent sensitivity in this energy range.

Another popular area of research that utilizes coherent x-ray diffraction imaging is biology, specifically, the 3D imaging of cells and viruses. Biological specimens contrast more weakly than nanoparticles, so soft x-rays in the 500 eV to 1 keV range are often used. Dr. Miao utilizes thermoelectrically or LN_2-cooled PI-SX cameras (now known as PIXIS-XO cameras) for imaging biological samples, again due to excellent sensitivity in the energy range of interest.

PI-LCX

High-sensitivity, megapixel PI-LCX cameras from Princeton Instruments (see Figure 4) feature special front-illuminated CCDs and high-resistance silicon to enable direct imaging of low-flux x-rays (< 3 keV to > 20 keV). An optional beryllium window design reduces low-energy background, whereas a rotatable ConFlat flange design provides a UHV hard-metal-seal interface that affords researchers the ability to image x-ray energy as low as 700 eV.

The camera's software-programmable, high-capacity or high-sensitivity amplifier allows the PI-LCX to offer x-ray photon counting capabilities with up to 16-bit dynamic range. A thermoelectrically cooled option provides maintenance-free operation, while an LN_2-cooled option ensures extremely low dark current for long exposures.

PIXIS-XO

High-sensitivity, megapixel PIXIS-XO cameras (formerly known as PI-SX cameras) from Princeton Instruments are equipped with special back-illuminated CCDs that lack anti-reflective coating, thus enabling direct imaging of low-energy x-rays (< 30 eV). A rotatable ConFlat flange design provides UHV hard-metal seals and the ability to align the CCD.

FIGURE 3.

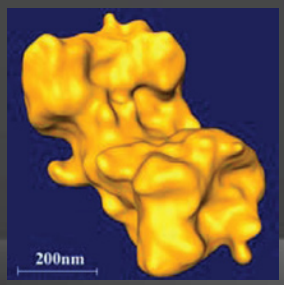

High-resolution 3D image of GaN particle created using coherent x-ray diffraction imaging. Image courtesy of Dr. Jianwei Miao, University of California, Los Angeles.

FIGURE 4.

Princeton Instruments PI-LCX cameras are optimized for direct imaging of medium x-rays.

Like the PI-LCX, the PIXIS-XO (see Figure 5) offers researchers x-ray photon counting capabilities with up to 16-bit dynamic range via a software-programmable, high-capacity or high-sensitivity amplifier. Also like the PI-LCX, a thermoelectrically cooled option provides maintenance-free operation, while an LN_2-cooled option ensures extremely low dark current for long exposures.

References

1. J. Miao, P. Charalambous, J. Kirz, and D. Sayre, "Extending the methodology of X-ray crystallography to allow imaging of micrometre-sized non-crystalline specimens", *Nature* **400**, 342-344 (1999).

2. J. Miao, T. Ishikawa, B. Johnson, E. H. Anderson, B. Lai, and K. O. Hodgson, *Phys. Rev. Lett.* **89**, 088303 (2002).

3. J. Miao, K. O. Hodgson, T. Ishikawa, C. A. Larabell, M. A. LeGros, and Y. Nishino, *Proc. Natl. Acad. Sci. USA* **100**, 110 (2003).

4. D. Shapiro, P. Thibault, T. Beetz, V. Elser, M. Howells, C. Jacobsen, J. Kirz, E. Lima, H. Miao, A. M. Neiman, and D. Sayre, *Proc. Natl. Acad. Sci. USA* **102**, 15343-15346 (2005).

5. M. A. Pfeifer, G. J. Williams, I. A. Vartanyants, R. Harder, and I. K. Robinson, *Nature* **442**, 63 (2006).

6. H. M. Quiney, A. G. Peele, Z. Cai, D. Paterson, and K. A. Nugent, *Nature Physics* **2**, 101 (2006).

7. H. N. Chapman *et al., Nature Physics* **2**, 839 (2006).

8. P. Thibault, M. Dierolf, A. Menzel, O. Bunk, C. David, and F. Pfeiffer, *Science* **321**, 379-382 (2008).

9. J. Miao, T. Ishikawa, T. Earnest, and Qun Shen, *Annu. Rev. Phys. Chem.* **59**, 387-409 (2008).

Resources

For more information about high-performance x-ray cameras from Princeton Instruments, please visit: **www.princetoninstruments.com**

For more information about Dr. Miao's research, please visit: **www.physics.ucla.edu/research/imaging**

FIGURE 5.

Princeton Instruments PIXIS-XO cameras are optimized for direct imaging of soft x-rays.

X-ray µCT Provides Nondestructive, High-Resolution 3D Imaging for Research and Industrial Applications

Introduction

Since the early 1970s, x-ray computed tomography (CT) has been one of the most versatile noninvasive investigative techniques in the medical field. It has also enabled nondestructive investigations in many other fields over the past few decades, including industry, archaeology, life science, geoscience, and crime investigations. Unfortunately, conventional x-ray CT systems are only able to achieve spatial resolution at the sub-millimeter scale. Thus, the technique is insufficient for examining the internal structure of objects that require resolution at the micrometer and nanometer scales.

X-ray computed microtomography (µCT), a more technologically advanced technique, overcomes this critical limitation via the use of high-resolution, wide-dynamic-range CCD cameras, high-resolution scintillators, either synchrotron x-ray sources or microfocus x-ray tubes, and software algorithms designed to reconstruct 3D images.

A typical µCT solution comprises an x-ray source, a high-resolution rotating stage with a sample holder, a high-performance scientific CCD camera, and a computer. Depending on the system configuration, either fiberoptic coupling or optical lens coupling is utilized to project an image onto the CCD detection array. Recent advances in all of the above-mentioned technologies enable spatial resolution on the order of microns (see Figures 1 and 2).

X-ray µCT at a Third-Generation Synchrotron Source

Extremely bright (i.e., high-flux) x-ray beams generated by synchrotron sources around the world are steadily increasing the utility of x-ray µCT in a number of research fields. Different configurations of x-ray beams (i.e., high-flux parallel beams or highly focused submicron beams) and high-resolution scintillators make it possible to extend the submicron scale, even below 100 nm, while maintaining reasonable data-acquisition times.

The work of geoscientist Dr. Mark Rivers of the University of Chicago provides an excellent example of the use of an x-ray µCT system at a third-generation synchrotron. In this particular µCT system, the transmitted x-rays are converted to visible light with a single-crystal YAG scintillator, which is imaged via either a microscope objective (5X to 20X) or a zoom lens, with the field of view adjusted between 3 mm and 50 mm. The image is then projected onto a CCD.

Dr. Rivers' data-collection software uses a layered approach in which each layer has a specific function. Data processing consists of preprocessing, sinogram creation, and tomographic reconstruction (see Figure 3).

FIGURE 1.

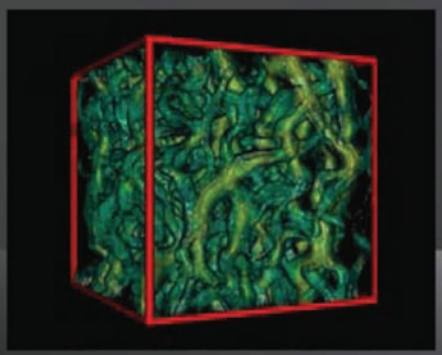

Simulated fluid streamlines through the pore space in a coral. Image courtesy of Dr. Tim Senden, ANU, Canberra, Australia.

FIGURE 2.

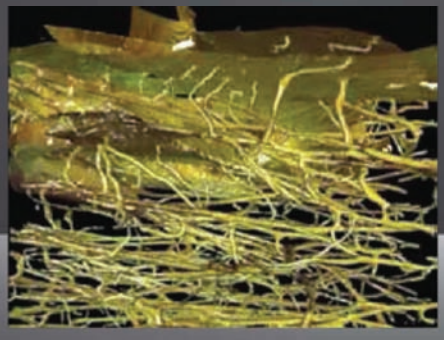

Human cortical bone showing Haversian and Volkmann's canals. Voxel size = 4 µm³. Image courtesy of Dr. Tim Senden, ANU, Canberra, Australia.

Optical lens-coupled µCT system

Photo courtesy of Dr. Yangchao Tian, NSRL, Hefei, P. R. China.

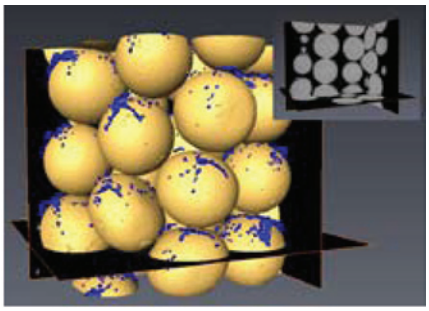

Figure 3. Glass beads (gold) with silver microspheres (blue). Image courtesy of Gabriel C. Iltis, Oregon State University, and Dr. Mark Rivers, University of Chicago.

The vast majority of x-ray µCT systems employed at third-generation synchrotron sources feature either a camera based on advanced electron-multiplying CCD technology (e.g., Princeton Instruments ProEM®) or a shutterless, interline-transfer CCD camera (e.g., Photometrics® CoolSNAP™ K4). These types of scientific cameras provide the high speed and outstanding sensitivity required for µCT experiments. Figures 4, 5, and 6 illustrate the technique's broad utility for performing work in diverse, complex fields such as materials science.

While third-generation synchrotron sources undoubtedly represent an extremely powerful research tool, limited access and expensive operation costs prove prohibitive to many scientists and industries. In the past several years, however, significant advancements in x-ray sources, detectors, sample stages, and computers have led to the design of "desktop" x-ray µCT systems that successfully bring a fair degree of this imaging performance to large and small labs alike.

FIGURE 4.

Nanoparticle image courtesy of Dr. Yangchao Tian, NSRL, Hefei, P. R. China.

FIGURE 5.

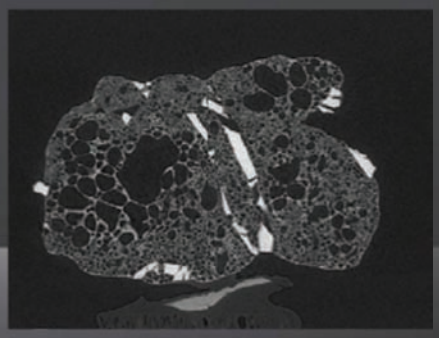

Lava synthesized at high temperature. Image courtesy of Liping Bai and Don Baker, Earth and Planetary Sciences, McGill University, Montreal, Canada, and Dr. Mark Rivers, University of Chicago.

Fiberoptic-coupled µCT system

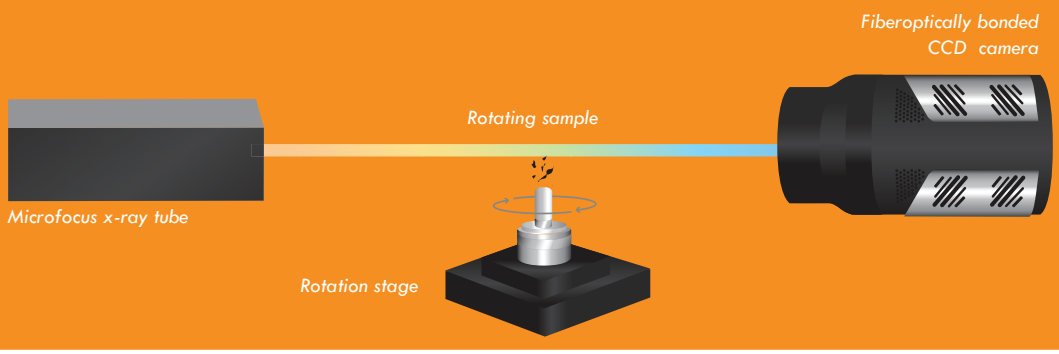

Desktop X-ray µCT with a Microfocus X-ray Tube

Instead of relying on an x-ray synchrotron source, desktop µCT systems use a microfocus x-ray tube with a focal spot size of less than 1 µm to achieve spatial resolution of features smaller than 100 nm. This emergent class of desktop systems embodies improvements in x-ray resolution, easy-to-use instrumentation, application flexibility, and affordability.

There are two fundamental kinds of desktop x-ray µCT systems. One uses fiberoptic coupling to project an image onto the CCD, whereas the other utilizes optical lens coupling. If high speed is important in an application (e.g., exposure times of 1 to 10 seconds), then a fiberoptic-coupled system is generally considered advantageous.

The images in Figures 7 and 8 were acquired with a fiberoptic-coupled desktop µCT system. To accommodate higher x-ray flux, fiberoptic-coupled desktop µCT systems can use fast-readout, high-sensitivity CCD cameras (e.g., Princeton Instruments Quad-RO, Princeton Instruments PIXIS-XF, and Princeton Instruments Nano-XF).

For x-ray imaging applications that require longer exposure times (e.g., 10 to 30 seconds, or even up to a few minutes), a high-sensitivity detector that can be deeply cooled to reduce dark current is essential. The utilization of Fresnel zone plates to focus the x-rays via diffraction onto the sample allows the use of optical lens coupling in the µCT system, which in turn necessitates deeper cooling of the detector.

FIGURE 6.

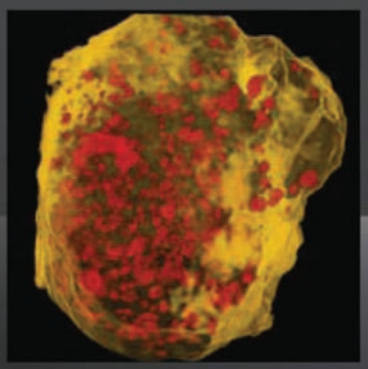

PCL-TCP-PLA sample. Voxel size = 0.7 µm³.
Image courtesy of Prof. M. Cholewa, SSLS, Singapore.

To preserve sensitivity and spatial resolution, optical lens-coupled desktop µCT systems often employ cooled cameras designed with megapixel, high-quantum-efficiency CCDs (e.g., Princeton Instruments PIXIS:1024B/F and 2048B/F).

Conclusion

The use of x-ray µCT systems in conjunction with third-generation synchrotron sources has facilitated advances in many research fields (e.g., materials science, geoscience, archaeology, life science, and drug discovery via small-animal CT) by offering truly remarkable performance, but appreciable expenses and tight scheduling bar many from this means of exploration. Over the past few years, hundreds of new desktop x-ray µCT systems from several manufacturers have been installed in labs around the world. These systems, which rely on microfocus x-ray tubes instead of synchrotron sources, represent an ongoing trend towards miniaturization and personalization of research technology.

Ongoing improvements in x-ray optics, sample stages, and scientific detectors continue to pave the way for new scientific breakthroughs (e.g., the development of electronic packages and more efficient fuel cells). In addition, the intelligent fusion of x-ray phase-contrast imaging and µCT techniques will open still more doors for researchers, enabling the imaging of extremely low absorption materials as well as delivering tools to diagnose cancer at even earlier stages.

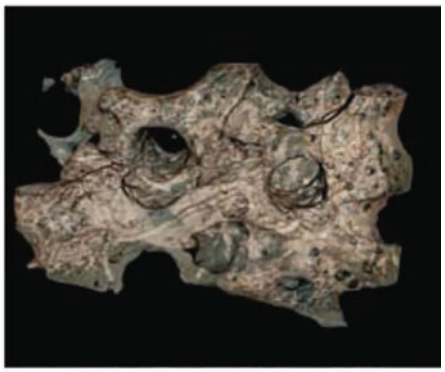

Figure 7. Tissue-engineered bone from a pig orbital reconstruction. Voxel size = 1.6 µm³. Image courtesy of Dr. Tim Senden, ANU, Canberra, Australia.

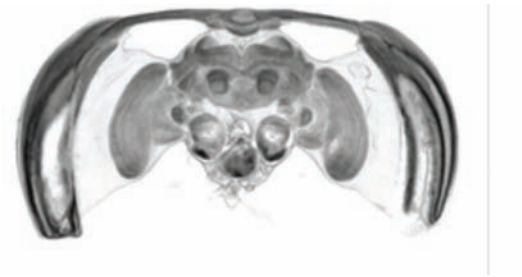

Figure 8. Bee brain. Image courtesy of Dr. Tim Senden, ANU, Canberra, Australia.

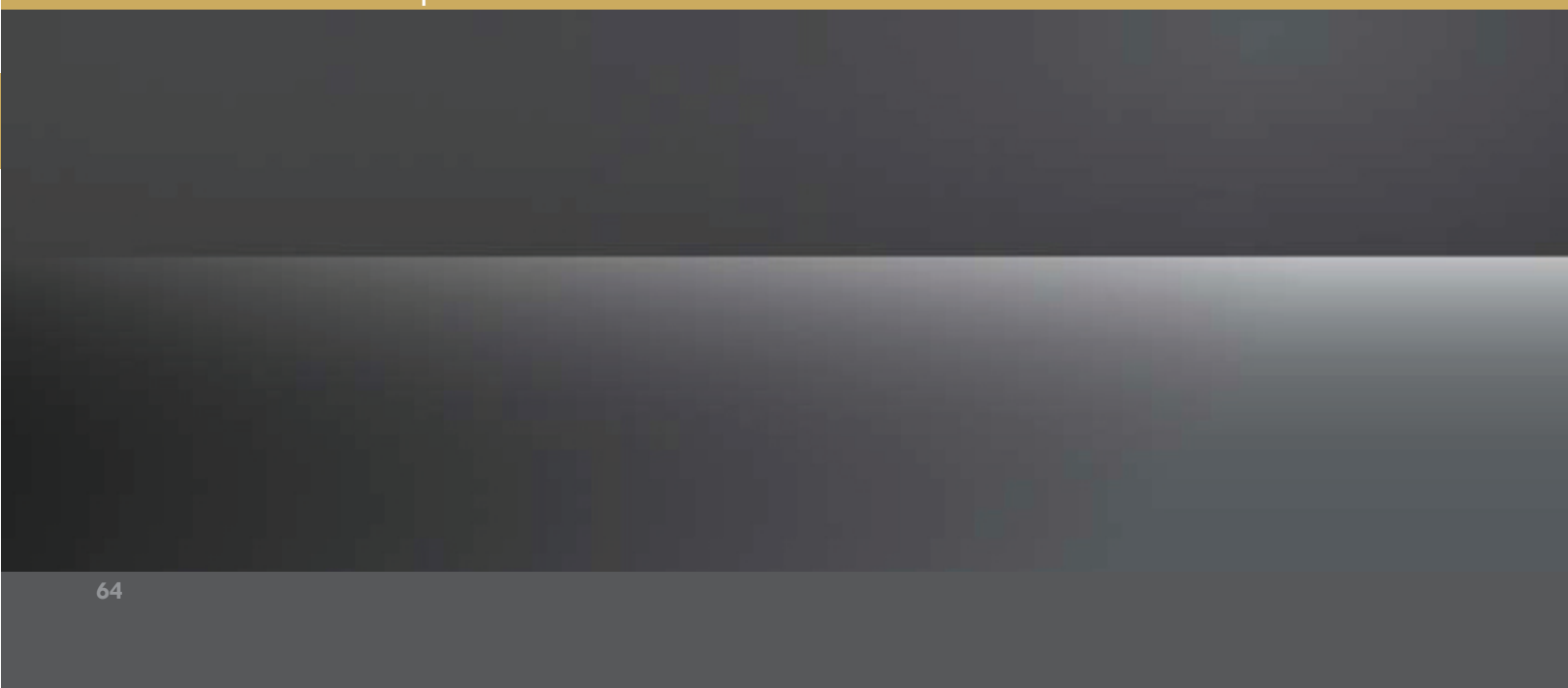

TECHNICAL NOTES

www.princetoninstruments.com

Flexible Electronic Architecture Extends Utility of Scientific Cameras

Introduction

Ultimately, the true worth of a scientific camera is determined by its ability to flexibly meet the performance requirements deemed most useful by a given researcher. As many disciplines have continued to evolve over recent years to encompass more varied investigatory techniques, sets of critical requirements have also expanded. When seeking a scientific camera to satisfy diverse needs, one must be sure to look for the most versatile, highest performance solutions available.

This note addresses some of the ways in which the flexible electronic architecture of Princeton Instruments scientific cameras extends application utility to facilitate research in a number of fields. The unique design of these CCD cameras features a pair of output amplifiers, each with its own software-selectable speed and gain settings, thereby enabling researchers to tailor performance to suit various x-ray, imaging, and spectroscopy applications.

Dual-Amplifier Design

Princeton Instruments' exclusive dual-amplifier configuration provides two independent amplifiers whose electronics are optimized for high-capacity readout and high-sensitivity readout, respectively. See Figure 1.

The high-capacity amplifier affords wider dynamic range by increasing full well capacity, in effect allowing each pixel of the CCD array to collect a greater number of photons. Generally speaking, the high-capacity amplifier is utilized for applications involving medium-energy x-rays or high levels of incident light.

The high-sensitivity amplifier, meanwhile, is designed to deliver the lowest possible read noise at a given readout frequency. Typically, the high-sensitivity amplifier is utilized for applications involving low-energy x-rays or low levels of incident light.

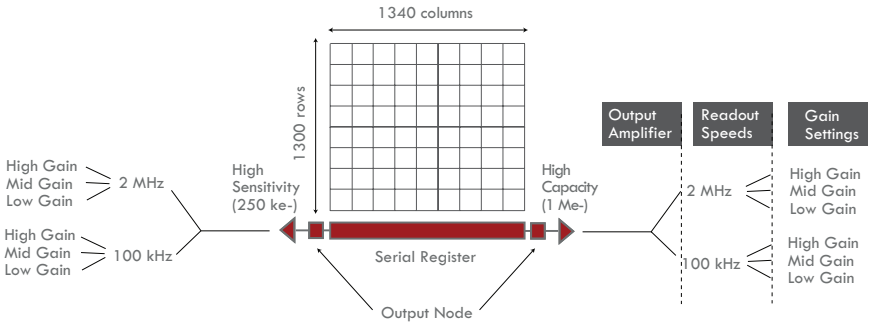

Figure 1. Two independent amplifiers optimized for high-capacity readout and high-sensitivity readout, respectively, extend CCD camera utility.

Selectable Speed and Gain

Both the high-capacity amplifier and the high-sensitivity amplifier offer their own independent, software-selectable speed and gain settings to allow researchers to fine-tune camera performance. Faster readout speeds can be used to acquire images quickly when the amount of incident light or energy is sufficient to do so without compromising results, or when setting up an experiment in focus mode. Slower readout speeds deliver high sensitivity by preserving dynamic range and boosting signal-to-noise ratio (SNR).

Note that signal-to-noise ratio refers to the relative magnitude of the signal compared to the uncertainty in that signal on a per-pixel basis. Specifically, it is the ratio of the measured signal to the overall measured noise (frame-to-frame) at that pixel. Accurate calculation of SNR must take into account the three primary sources of noise in a CCD camera (i.e., photon-flux-related shot noise, thermally generated dark noise, and the aforementioned read noise) as well as several additional noise sources. High SNR is particularly important in applications requiring precise light measurements.[1]

Like selectable readout speeds, selectable gain settings also provide researchers a valuable tool for tailoring camera performance. Gain defines the number of electrons that correspond to a single analog-to-digital unit (e-/ADU). For example, a gain of 4 means the camera digitizes the CCD signal so that each ADU corresponds to 4 electrons. Prior to the application of gain, each photon detected by the CCD generates a given number of electrons based on the photon's energy.

Soft X-ray Applications

Soft x-rays have photon energies between 100 eV and 1000 eV (12.4 nm to 1.24 nm). These wavelengths allow researchers to utilize high-spatial-resolution x-ray microscopy techniques that offer good penetration in micrometer-thick specimens without the laborious sample preparation required by transmission electron microscopy. Soft x-rays also enable elemental analysis of specimens by providing excellent intrinsic contrast between organic materials (e.g., proteins) and water in the so-called "water window" (284 eV to 543 eV) between the carbon and oxygen absorption edges.

At 250 eV, only 68.5 electrons are generated for each photon detected by the CCD; at 100 eV, just 27.4 electrons are generated per detected photon. Thus, when working with soft x-rays, the high-sensitivity amplifier should be utilized. Slower speed settings can further enhance sensitivity. In addition, the high-sensitivity amplifier's gain settings should be used to optimize dynamic range and SNR to achieve the image contrast required. The x-ray energy itself can also be tuned to attain desired contrast.

Princeton Instruments recommends megapixel PIXIS-XO cameras for working with soft x-rays. These scientific cameras are equipped with special back-illuminated CCDs that lack anti-reflective coating, thus enabling direct imaging of very low energy x-rays (< 30 eV). A rotatable ConFlat flange design provides UHV hard-metal seals and the ability to align the CCD.

PIXIS-XO camera with rotatable ConFlat flange.

Hard X-ray Applications

Hard x-rays have photon energies greater than 1000 eV (1 keV). One increasingly popular x-ray imaging application in this range is *coherent x-ray diffraction imaging,* also known as *lensless x-ray diffraction imaging*. In this technique, a CCD camera is used to detect the continuous diffraction pattern that results from shining a pink x-ray beam on a noncrystalline specimen. Use of coherent x-ray diffraction imaging is expanding from the soft x-ray range (for imaging biological specimens) into the 5 keV to 7 keV range (for imaging nanoparticles).[2] See Figure 2.

Another application that uses hard x-rays is *x-ray photon correlation spectroscopy,* or *XPCS*. In this technique, fluctuations in frequency and intensity of the scattered light (caused by temperature and pressure changes) in a sample are imaged at 8 keV. See Figure 3.

Even at 1 keV, around the lower boundary of the medium-energy x-ray range, 274 electrons are generated for each photon detected by the CCD. Therefore, since additional sensitivity is not required to boost SNR, researchers should utilize the high-capacity amplifier when working with hard x-rays. Slower readout speeds and higher gain settings are typically less beneficial in this energy range due to the already sufficient sensitivity and ample signal.

Princeton Instruments recommends megapixel PI-LCX cameras for working with hard x-rays. These scientific cameras feature special front-illuminated CCDs and high-resistance silicon to enable direct imaging[3] of low-flux x-rays (< 3 keV to > 20 keV). An optional beryllium window design reduces low-energy background, whereas a rotatable ConFlat flange design provides a UHV hard-metal-seal interface that affords researchers the ability to image x-ray energy as low as 700 eV.

Astronomical Imaging

Within the remarkably broad realm of scientific imaging, astronomy applications are especially noteworthy for the stringent demands they often make on advanced imaging instrumentation. One example of such an application is the near-infrared imaging of the sun's outer corona during a solar eclipse lasting a few minutes. See Figure 4.

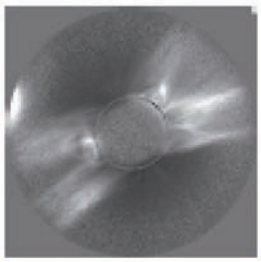

Figure 4. Sun's outer corona captured during a solar eclipse using a PIXIS:1024BR camera. Image courtesy of Dr. Shadia Habbal, Institute for Astronomy, University of Hawaii, Honolulu.

In addition to the many technical challenges associated with the fleeting window of opportunity afforded by this rare phenomenon, there is also the need to use relatively long exposure times (~ 1 min) to capture the limited available signal. For this type of application, Princeton Instruments recommends back-illuminated (high-QE) megapixel PIXIS scientific cameras. Using the high-sensitivity amplifier in conjunction with high gain and slow readout speed raises SNR. The deep thermoelectric cooling of the PIXIS further increases SNR by greatly reducing the thermally generated dark noise that accumulates during exposures.

FIGURE 2.

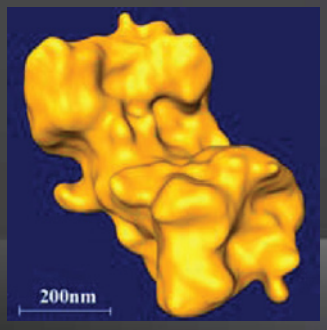

High-resolution 3D image of GaN particle created using coherent x-ray diffraction imaging. Image courtesy of Dr. Jianwei Miao, University of California, Los Angeles.

FIGURE 3.

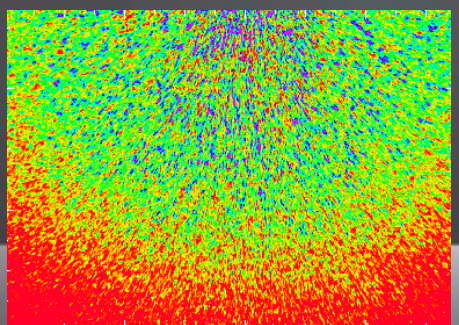

Small-angle scattering from an aerogel using XPCS. Image courtesy of Dr. Alec Sandy, Advanced Photon Source, Argonne National Laboratory.

For photon-starved applications that require even longer exposure times, Princeton Instruments recommends back-illuminated (high-QE) megapixel Spec-10® scientific cameras. The liquid nitrogen cooling of the Spec-10 minimizes thermally generated dark noise for exposure times on the order of hours.

Researchers working in the near-infrared range should note that many Princeton Instruments scientific cameras can be configured with deep-depletion CCDs. These devices utilize a bias voltage applied to a thick layer of high-resistivity silicon in order to produce a "deeper" depletion region (active photosensitive area) than that of conventional CCDs. This architecture allows longer-wavelength photons to interact within the layer as opposed to merely penetrate it.

Raman Spectroscopy

Raman spectroscopy, a highly popular technique for studying solids, liquids, and gases, is based on the scattering of monochromatic light. Excitation light (usually from a laser) is absorbed by a sample and then re-emitted; the resultant "Raman shift" provides information on vibrational, rotational, and other molecular modes. See Figure 5.

Since the pixel binning employed for this photonstarved application increases noise as well as signal, the high-sensitivity amplifier should be used along with slower readout speeds and medium-to-high gain to boost SNR while preserving wide dynamic range.

To minimize the accumulation of thermally generated dark noise during Raman spectroscopy's rather long exposures, Princeton Instruments recommends a back-illuminated (high-QE) Spec-10:400 scientific camera with liquid nitrogen cooling. For spectroscopy applications requiring shorter exposure times, Princeton Instruments recommends a back-illuminated (high-QE) PIXIS:400 scientific camera with deep thermoelectric cooling.

Conclusion

The flexible electronic architecture of Princeton Instruments scientific cameras provides two distinct output amplifiers designed for optimum highcapacity and high-sensitivity readout, respectively. Camera performance can be further refined using each amplifier's software-selectable speed and gain settings.

This built-in versatility allows researchers to utilize an individual scientific camera for a greater range of applications without sacrificing high performance.

Spec-10:400 camera with liquid nitrogen cooling.

PIXIS:1300 camera with deep thermoelectric cooling.

FIGURE 5.

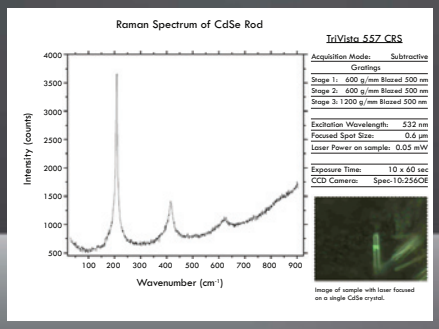

Raman spectrum of CdSe rod acquired using a Spec-10:256 camera and a Princeton Instruments TriVista™ confocal Raman microscope system (CRS).

REFERENCES

1. "Keep the noise down! Low noise: an integral part of high-performance CCD (HCCD) camera systems", Princeton Instruments technical note (1999).

2. "Coherent x-ray diffraction imaging", Princeton Instruments x-ray application note (2009).

3. "Direct detection of x-rays (4 keV to ~ 20 keV) using detectors based on deep-depletion CCD technology", Princeton Instruments technical note (2000).

Direct Detection of X-rays (30 eV to 20 keV) Using Detectors Based on CCD Technology

Introduction

Since their introduction in 1969, charge-coupled devices (CCDs) have become increasingly specialized to meet the changing requirements of both commercial and scientific markets. In the scientific market, CCDs have been improved and optimized in a variety of ways to provide high performance across a broad set of applications — from spectroscopy and semiconductor testing to biological imaging and genetic research. The wider dynamic range, superior sensitivity, better linearity, and real-time response of CCDs have helped these devices replace traditional imaging methods, such as film.

Design modifications to scientific-grade CCDs, initially driven by interest in x-ray astronomy applications, have greatly expanded the domain of x-ray imaging and x-ray spectroscopy. Devices have been engineered to detect x-rays in the energy range extending from well below 100 eV all the way up to 100 keV and higher (a full three orders of magnitude), making them invaluable for research in which high sensitivity is combined with two-dimensional detectors.

These devices are utilized in many x-ray techniques, including x-ray microscopy, x-ray lithography, x-ray intensity fluctuation spectroscopy, x-ray crystallography, medical x-ray imaging, and x-ray nondestructive testing. Figure 1 lists recommended CCD camera technologies for various energy ranges.

In direct-detection cameras, the CCD is directly exposed to the incoming x-ray photons, which enables direct absorption (i.e., detection) of the photons. Depending on the x-ray energy range, either a back-illuminated CCD without anti-reflection (AR) coating, or a front- or back-illuminated, deep-depletion CCD is used.

Basic Principles

When exposed to visible light (380 nm to 750 nm), front- and back-illuminated CCDs generate a single electron-hole pair in the epitaxial layer for each absorbed photon. The optimal epitaxial-layer thickness required to achieve the highest quantum efficiency (QE) in these devices varies with wavelength. To attain the best overall results, manufacturers of front- and back-illuminated CCDs have settled on standard thicknesses of approximately 20 µm and 15 µm, respectively.

Although these standard epitaxial-layer thicknesses can absorb x-rays in the range from approximately 30 eV to 20 keV (see Figure 2), other components within the CCD help dictate the type of device needed to detect low- and medium-energy x-rays.

FIGURE 1.

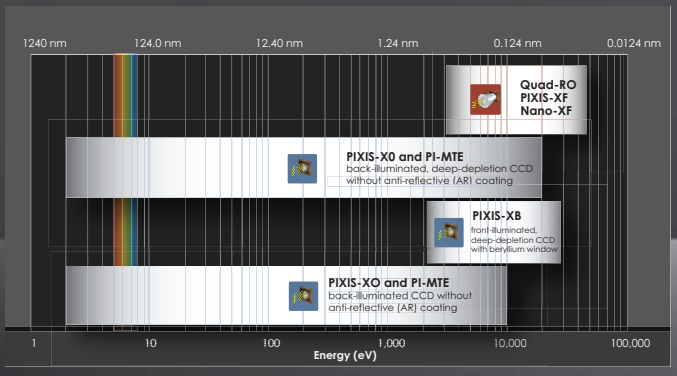

CCD camera technologies recommended for various x-ray energy ranges.

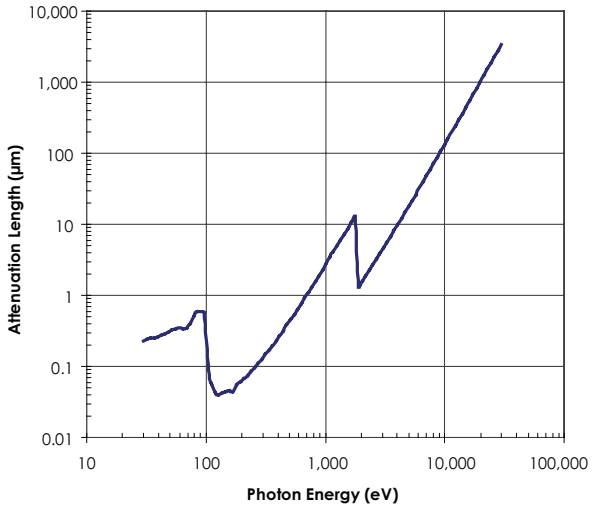

Figure 2. X-ray attenuation length at various energy levels.

For instance, because both the electrode structure and the insulating layer of a front-illuminated CCD will absorb x-ray photons below energies of 700 eV, a back-illuminated CCD architecture is required to detect low-energy x-rays (about 30 eV to 3 keV). The cross section of a back-illuminated CCD is shown in Figure 3a.

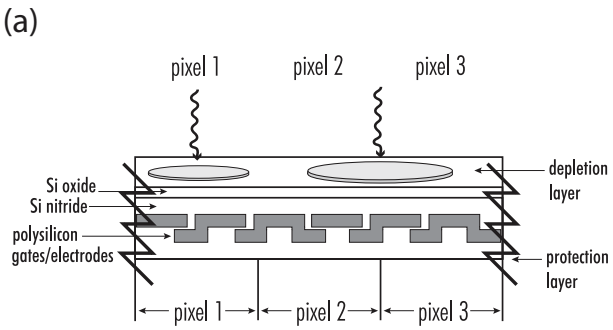

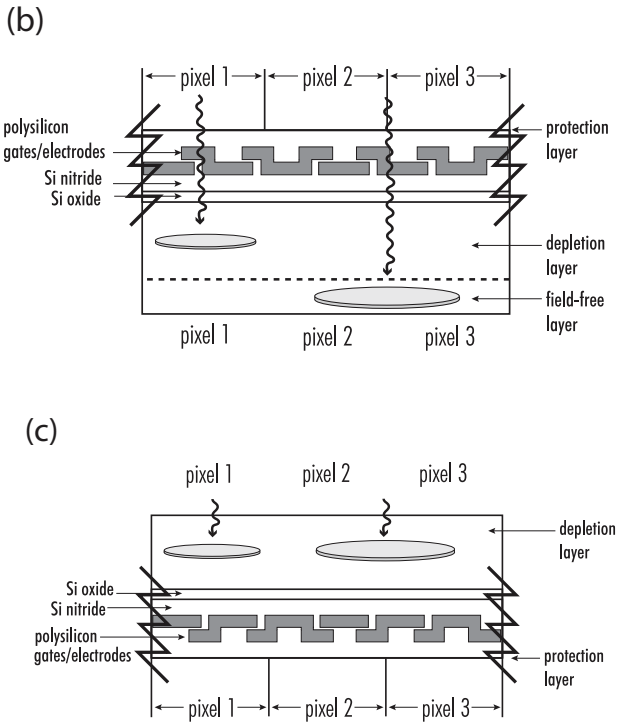

Figure 3. Cross sections of the three primary CCD architectures used for the direct detection of x-rays: (a) back-illuminated CCD; (b) front-illuminated, deep-depletion CCD; and (c) back-illuminated, deep-depletion CCD.

When it comes to "extremely low energy" x-rays (approximately 30 eV to 500 eV) even AR coating itself can absorb x-ray photons. With this in mind, Princeton Instruments designed its PIXIS-XO and PI-SX direct-detection cameras using back-illuminated CCDs without AR coating (see Figure 4). These cameras also feature a rotatable ConFlat flange that provides a UHV hard-metal-seal interface. It should be noted that for medium-energy x-rays (about 3 keV to 20 keV), back-illuminated CCDs with or without AR coating can be used, although the QE may prove to be a limitation.

FIGURE 4.

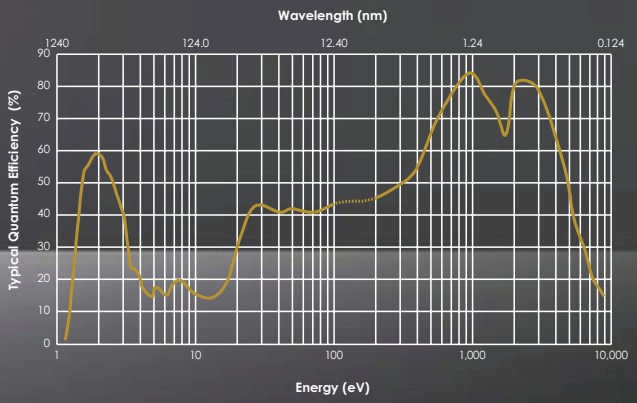

A typical QE curve for a back-illuminated CCD.

To meet the demand for higher QE in the medium-energy x-ray range, CCD manufacturer e2v developed front-illuminated, deep-depletion technology several years ago as a way to increase sensitivity. To achieve a favorable balance between QE, spatial resolution, and blemishes, e2v utilizes a 50 µm-thick epitaxial layer for these devices (Figure 3b).

Figure 5 shows a typical QE curve for a front-illuminated, deep-depletion CCD. To optimize detector QE, Princeton Instruments PIXIS-XB and PI-LCX cameras utilize these CCDs in conjunction with a beryllium window, a design that gives researchers the freedom to use the camera in the lab without having to attach the detector to the vacuum chamber.

For extremely demanding applications that require x-ray sensitivity spanning the low-to-medium energy range (about 30 eV to 20 keV), Princeton Instruments has also designed a PIXIS-XO camera that uses a back-illuminated, deep-depletion CCD (Figure 3c) without AR coating. This camera features a rotatable ConFlat flange, but alternatively it can be supplied with a removable ConFlat flange with a beryllium window.

Finally, for ultimate operational flexibility within the vacuum chamber, Princeton Instruments offers the PI-MTE camera, which can be delivered with any of the aforementioned CCDs.

Charge-Generation Mechanism

X-ray photons traveling through the layers of a CCD can lose energy through Compton scattering, fluorescence, or the photoelectric effect. For energies less than 150 keV, the photoelectric effect is dominant. Thus, when an x-ray photon in the 30 eV to 20 keV energy range is absorbed in the silicon, its energy is converted via the photoelectric effect and generates electron-hole pairs in the CCD based on the primary x-ray photon energy.

To produce one electron-hole pair in silicon, an x-ray photon requires an average of 3.65 eV per pair. Therefore, when an x-ray photon of 8.0 keV is absorbed it generates about 2192 e- (8000/3.65). Note that fluctuations in the average energy required to produce an electron-hole pair are governed by the interaction of x-ray photons within the silicon. These fluctuations are summarized by a numerical factor called the Fano factor. The Fano factor for silicon is about 0.1. The effect of Fano factor on system noise and energy resolution is beyond the scope of this discussion.

Charge-Collection Mechanism

For scientific applications that place a high premium on quantitative measurements, it is important that the charge generated by an x-ray photon is collected within one pixel and then transported to the output amplifier without suffering losses from imperfect charge-transfer efficiency (CTE). Depending on its generation locale, there is some probability that the photoelectron charge cloud will be split between two or more pixels. This level of uncertainty must be accounted for in order to ensure the most accurate data.

FIGURE 5.

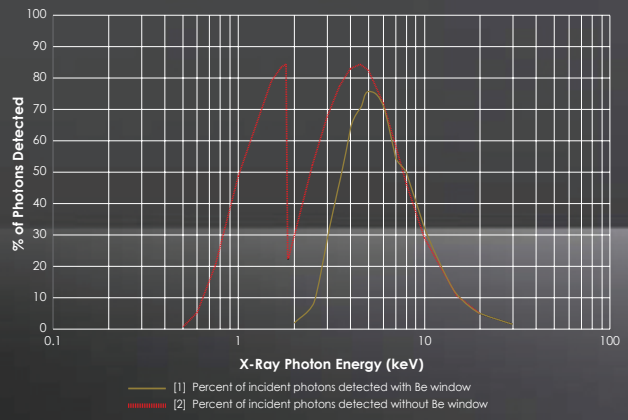

A typical QE curve for a front-illuminated, deep-depletion CCD.

If the charge is generated in a field-free layer, then it moves by diffusion and either recombines or reaches the edge of the depletion layer field. Any charge that reaches (or is generated within) the depletion layer is swiftly drifted to the surface collection site with minimal radial spread. Charge that is generated close to the edge of a pixel, or deep in the substrate, can split between pixels. Some charge from deeply generated events may also recombine so that the charge is not conserved.

The measurement of signal charge does not always indicate the true deposited energy, particularly for events generated deep in the CCD (high-energy x-rays in the case of a front-illuminated device). Some partial events may also be evident in a pulse height distribution generated from a monochromatic x-ray source.

In a back-illuminated device, in which the field-free layer is etched out, the electrons are generated directly in the epitaxial layer. Therefore, in this case, migration of generated electrons can also occur in lower-energy x-rays, as they are generated near the surface.

When the detector is used in a photon-counting mode, steps should be taken to ensure that (1) the incoming flux, related to the exposure time, is weak enough to prevent multiple x-ray photons from reaching the same pixel and (2) a method to differentiate single-pixel events from multiple-pixel events has been implemented in the system. See Figure 6.

Typically, an intensity-threshold method is used to distinguish between single-pixel and multiple-pixel events. To utilize this method, precise threshold levels for single-pixel events and multiple-pixel events must be selected, as illustrated in the following example.

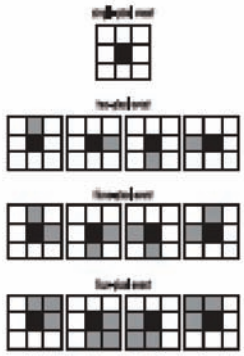

Figure 6. An example of single- and multiple-pixel events. The dark pixels represent the counts above the single-pixel threshold and the shaded pixels show the counts between the single-pixel and multiple-pixel thresholds.

Example

For an Fe^{55} source and a CCD with gain calibration of 6 e-/ADU (analog-to-digital unit), the single-pixel-event threshold can be set between 230 and 300 ADUs, and the multiple-pixel-event threshold can be set between 50 and 175 ADUs.

Fe^{55} = 5.898 keV; CCD gain calibration = 6 e-/ADU; 3.65 eV = 1 e-

Single-pixel-event intensity = 5898/(3.65*6) ≈ 269 ADUs

Multiple (two)-pixel-event energy = 269/2 ≈ 135 ADUs

Multiple (maximum four)-pixel-event energy = 269/4 ≈ 67 ADUs

If a single pixel has an intensity that is greater than the upper limit of the single-pixel-threshold level, it can be treated as two photon events.

Radiation Damage

Unfortunately, the good sensitivity and higher quantum efficiency attained with CCDs designed for direct x-ray detection comes with an inherent tradeoff. That is, once a significant quantity (i.e., dose/flux) of x-ray radiation has bombarded the CCD, permanent damage occurs. In particular, the following changes in performance parameters are observed:

- Increase in dark current
- Flat-band voltage shift
- Reduction in CTE (critical for x-ray spectroscopy)

These parameters are affected differently by various types of radiation — namely protons, neutrons, and heavy ions (energetic particles), as well as electrons, gamma rays, beta rays, and x-rays (ionizing radiation). Performance degrades slowly as the dose of ionizing radiation builds up, but very rarely reaches the catastrophic levels that can result in sudden failure. Therefore, the specific radiation dose that marks the end of useful life can vary widely depending on the application, the x-ray energy, and the radiation flux. Some of these effects are intrinsic to all silicon-based devices, but others are related to CCD structures and manufacturing processes.

Increase in Dark Current

As x-ray photons strike the silicon, they create additional interface states between the silicon and the silicon-dioxide gate oxide. Since these new states have energy levels within the silicon band gap, they then lead to an increase in dark current.

Flat-Band Voltage Shift

When x-rays are absorbed in the gate oxide, electron-hole pairs are generated. Some of the electrons are detected as signal, some of them recombine, and the remaining electrons escape from the oxide. The mobility of the holes, however, is much lower than that of the electrons; thus, some holes become trapped in the oxide.

These trapped holes result in a positive space-charge buildup that modifies the gate potential and increases the potential in the active region of the epitaxial silicon. The effect is referred to as a flat-band voltage shift.

If the charge buildup becomes too large, the CCD clock and bias voltages may have to be adjusted to maintain device performance.

Reduction in CTE

If the energy of the radiation is high enough, displacement damage will occur in the silicon lattice. In turn, CTE will be diminished. To displace silicon atoms, electron kinetic energy of approximately 150 keV is required — so this effect is negligible for the x-ray energies under discussion here.

In back-illuminated CCDs, incident photons reach the epitaxial layer before encountering the gate structure. Therefore, radiation damage does not occur at energy levels that fall below a device-specific threshold within the low-energy x-ray range. Even at energy levels where x-rays reach the electrode structure, radiation damage is delayed.

Annealing Damage

It has been reported that if a device with high dark current due to x-ray irradiation is treated in forming gas (10% H_2; 90% N_2) at about 350 °C for a few hours, the CCD's performance can be restored to its pre-irradiation level.

It has also been reported that if exposed to a 254 nm UV wavelength source (EPROM-erasure light source) for about 10 minutes, the shift in various voltages can be reduced.

Note that these treatments may render the CCD more susceptible to future x-ray damage. However, if the device is annealed at 100 °C for about 15 hours in air after the completion of the 350 °C-forming-gas annealing, then this effect may be countermanded.

None of the experiments listed in this section has been performed in Princeton Instruments' lab, therefore we strongly recommend that caution be exercised when attempting these procedures. Depending on the amount of damage to a specific CCD, either the temperature or the hours of exposure may have to be adjusted.

Direct- and Indirect-Detection Solutions

Scientific cameras designed for the direct detection of low- or medium-energy x-rays typically utilize a back-illuminated CCD without AR coating; a front-illuminated, deep-depletion CCD; or a back-illuminated, deep-depletion CCD.

In addition to these direct-detection solutions, Princeton Instruments offers a number of CCD cameras designed for the indirect detection of higher-energy x-rays via the use of fiberoptic inputs. These cameras include the Quad-RO, PIXIS-XF, and Nano-XF.

Please visit www.princetoninstruments.com for more information about advanced scientific cameras optimized for either the direct or indirect detection of x-rays.

Contact Princeton Instruments for additional information about advanced x-ray cameras!

Teledyne Princeton Instruments | Main Office- (USA)
Tel: +1 609.587.9797 | pi.info@teledyne.com

TELEDYNE
PRINCETON INSTRUMENTS
Everywhereyoulook™

Part of the Teledyne Imaging Group